Modelling and Simulation of Hybrid Electric Trains Powered by Hydrogen Fuel Cells and Batteries for Routes in the Highlands of Scotland

Preliminary results

A Report for the Scottish Association for Public Transport

David Murray-Smith

Honorary Senior Research Fellow
and Emeritus Professor of Engineering Systems and Control,
James Watt School of Engineering, University of Glasgow

Email: David.Murray-Smith@glasgow.ac.uk

27th June 2020

Abstract: This report builds on an earlier review for the Scottish Association for Public Transport on the potential of batteries, hydrogen fuel cells and other short-term energy storage systems for railway and tramway applications. It outlines the development of a train performance model and associated computer simulation software for a design of hybrid multiple unit, powered by a combination of hydrogen fuel cells and batteries. Assumptions underlying the model are discussed in detail. The chosen mode of operation involves steady state conditions for the fuel cells, with the batteries being used to provide additional stored energy for use on gradients and when the train is accelerating. The simulation techniques involve a mix of conventional "forward" simulation and an approach based on an "inverse" simulation method.

Simulation results presented are for a case study involving a short section of route chosen to be typical of sections of many rural routes in Scotland, such as the West Highland lines and routes north and west of Inverness or to and from Stranraer. Data relating to the performance of Class 156 diesel multiple units currently used on non-electrified railway lines in Scotland have provided a point of reference in assessing the performance of the hybrid multiple units. Although other studies of hybrid rail vehicles involving hydrogen fuel cell and battery combinations have been published, those have involved routes that are shorter, with more intermediate stations and no prolonged gradients.

Conclusions are presented in terms of fuel cell and battery power levels and battery storage capacity required for operation on the type of route being considered. The most important conclusion is that a preliminary specification for a hybrid two-coach unit could involve two 200 kW traction motors, fuel-cells providing a maximum power output of 350 kW and a battery pack giving a maximum power output of 250 kW and 75 kWh of electrical energy storage capacity. Using standard components that are available commencially, approximate calculations suggest that a design based around these power ratings could be implemented within a target weight of 90 tonnes for a two-coach unit. However, it is thought that the limitations of the UK loading gauge could present difficulties in terms of the space required and implementation might only be possible at the cost of some passenger space. Suggestions are made in the report for further simulation work involving a three-coach configuration and for the addition of a pantograph and associated electrical equipment to allow power to be drawn from 25 kV overhead wiring when the unit is operating on electrified routes. Another important recommendation for further work involves development of a detailed route model for a typical line, including exact information about gradients, curvature and local speed restrictions. Assessment of possible journey-time reductions is also important and preliminary results are presented, for the specification given above, using inverse simulation methods. Potential journey-time reductions over a complete route or specific sections could be investigated in future work. Issues of weight could also be linked to performance within the simulation software and advice could be provided to the user when space or weight constraints are violated.

The report includes discussion of possible benefits of developing more detailed, physics-based, sub-models of elements such as fuel cells, batteries, traction motors and power electronic components which could be used to replace the much simpler sub-models used in the existing simulation model. This might allow use of well-established and validated sub-models and would extend the range of issues that could be addressed through simulation and allow more accurate assessment of losses in batteries, power electronic components and traction motors over the full range of operating conditions. This could also be of value for checking underlying assumptions within the model and for the development of control and energy management strategies. The report recommends the use of both forward and inverse methods of simulation for applications of this kind as these two approaches, taken together, can provide additional insight that is not obtained so readily from the use of conventional forward simulation methods alone.

Keywords: Rail traction; hybrid vehicles; electrical battery; hydrogen fuel cells; computer simulation; inverse simulation; railways in Scotland.

CONTENTS

1. Introduction

Growing concerns about exhaust emissions and their effects in terms of climate change and health issues make re-examination of our choice of transport modes a priority. The United Kingdom has amended the Climate Change Act 2008 to incorporate a reduction to zero of its net contribution to greenhouse gas emissions by 2050. The UK Department of Transport has recently published a policy paper explaining how it intends to develop a plan to meet this target for the transport sector [1]. As part of the work towards the 2050 goal, a Rail Industry Decarbonisation Taskforce was created in 2018 and recommendations have been made already to the UK Rail Minister that, if implemented successfully, could make the UK rail system the leading low carbon network in the world by 2040 [2]. In planning to phase out diesel traction within the next twenty years, a Traction Decarbonisation Network Strategy has been developed to inform Government decisions on further electrification and the use of other technologies and a report outlining options for traction energy decarbonisation has been produced [3]. Although electrification is recognised as a highly cost-effective alternative to diesel traction for heavily used inter-city routes, many regional routes lack the traffic density to support a successful business-case for conventional electrification.

Under the devolved administration in Scotland, transport issues are the responsibility of Transport Scotland, rather than the UK Department for Transport and the targets established as part of the Scottish Government's new National Transport Strategy are more ambitious than those set by the UK Government [4]. For example, the Scottish Government intends to phase out the need for new petrol and diesel cars in Scotland by 2032 and has set a target of net zero greenhouse gas emissions by 2045 at the latest, with interim reduction targets of 70% by 2030 and 90% by 2040. In the introduction to a key policy document *"Protecting Scotland's Future: the Government's Programme for Scotland 2019-2020"* the First Minister of Scotland has included a statement about her Government's intention to include commitments to "…reduce emissions from Scotland's railways to zero by 2035 through continued electrification of the network, the procurement of battery-powered trains and exploration of the potential of hydrogen-powered trains in Scotland" [5]. In this context it is interesting to note that there was an announcement in March 2020 that one of the withdrawn Class 314 electric multiple-units is to be converted to hydrogen power in a development programme led by Scottish Enterprise in conjunction with Transport Scotland and industrial partners [6].

Alternatives to traditional electric or diesel traction are not simply battery-electric vehicles and vehicles powered by hydrogen fuel cells. They must also include various hybrid configurations such as conventional electric traction with a secondary battery or diesel engine for use beyond the limits of the electrified network, various battery-electric and diesel combinations, hydrogen fuel cell and battery-electric configurations or systems based on other forms of energy storage. Such combinations are now recognised as being potentially important for a range of future railway applications.

1.1 A brief review of battery-electric power for rail traction

Battery power for rail transport is relatively well established and in the 1950s and 1960s battery-electric units were used quite widely in Germany. In Scotland, a battery-electric multiple-unit was developed in the late 1950s at the British Railways Cowlairs workshops in Glasgow and used on the Aberdeen to Ballater branch between 1958 and 1966. That involved a 46-mile route with some relatively short but sharp gradients and quite a demanding timetable. It should be noted that lead-acid batteries were used, weighing significantly more than equivalent modern batteries and occupying much more space [7], [8]. Well-publicised developments since that time include the experimental modification of a Class 379 electrical multiple unit by Bombardier for tests in 2018 involving battery-powered operation on the Manningtree to Harwich branch [9] and a successful demonstration by Vivarail of a two-car Class 230 battery-electric unit on the Bo'ness and Kinneil Railway [10], [11]. Other activities reported recently in the UK include rebuilding by Brush of a Class 319 electric multiple unit to include battery technology and similar work to convert Siemens Class 350/2 units into so-called *BatteryFLEX* trains [12]. Hitachi

has also made proposals to develop augmented Class 385 units, with battery power, for use on some non-electrified lines in Scotland [13]. In terms of firm orders for new trains there have been several developments in other European countries, one example being the announcement by Bombardier and Austrian Federal Railways (ŐBB) of an order for 25 *Talent 3* six-coach units for regional services, with the battery system being charged from overhead wires on electrified sections or from charging points at terminal stations [14].

Limiting factors in terms of the use of battery propulsion include restricted range, cost, provision of the necessary re-charging infrastructure and long-term problems of materials-sourcing, manufacture and disposal. Weight is another important issue and it is interesting to note that the battery units on the Class 379, which was modified by Bombardier for the tests in East Anglia in 2018, reportedly weighed 8 tonnes including metal rafts for housing. However, batteries remain attractive because of the low capital cost compared with conventional electrification or the provision of expensive refuelling installations for hydrogen trains. Bi-mode battery/electric trains may be well suited for use on routes involving a mixture of electrified and non-electrified sections but the limited operating range between re-charging points makes such trains inappropriate for routes such as the West Highland lines. Increasing the battery storage capacity to extend the range introduces weight penalties that have a detrimental effect on performance.

1.2 A review of hydrogen fuel-cell technology for rail traction

Rail applications of hydrogen fuel cell technology are still uncommon. One reason is that the production of hydrogen fuel is relatively costly compared with other sources of energy. At present, hydrogen production involves either a "reforming" process from natural gas (with the disadvantage of producing some greenhouse gas emissions) or by electrolysis, using standard electricity supplies or dedicated electricity supplies from renewable sources. Unfortunately, currently available hydrogen fuel cells do not respond quickly to demanded changes of power level and are not reversible. They are best used under steady-state conditions where they supply electricity to a battery (or other electrical energy storage element) which, in turn, supplies the traction motors and other on-board electrical systems. Most present-day transport applications of hydrogen fuel cells involve hybrid systems incorporating a battery within the powertrain.

Much published material on the engineering aspects of alternative forms of power for rail vehicles comes from a small number of large university research groups specialising in railway topics. These include groups at Imperial College in London (Transport Strategy Centre and Future Railway Research Centre)), the University of Southampton (Southampton Railway Systems Research), the University of Birmingham (Birmingham Centre for Railway Research and Education (BCRRE)) and the University of Huddersfield (Institute of Railway Research). Several smaller research groups exist at other UK universities and these are also making important contributions in several areas. The BCRRE group at the University of Birmingham is particularly significant in the context of this report since it is the lead university partner within the UK Rail Research and Innovation Network. BCRRE will also soon host the newly established Centre of Excellence in Rail Decarbonisation [15].

One of the most-detailed published investigations of the potential of hydrogen powered rail vehicles in the UK describes results of collaborative design work involving partners from the University of Birmingham, Hitachi Rail and Fuel Cell Systems Ltd. A report [16] from those organisations, published in 2016, presents results of quantitative analysis concerning a fuel-cell based powertrain intended for retrospective fitting to diesel multiple-units or for new regional multiple-units. Examples considered included a Class 156 diesel multiple-unit and versions of Hitachi's AT200 electric multiple-unit (such as the Class 385 electric multiple units in service in Scotland). Two configurations were considered in that report, one involving the use fuel-cell power directly, with no battery within the powertrain, while the second configuration was a hybrid system with a battery that could be charged through regenerative braking or from the fuel cell while the unit was coasting, in the cruise mode or at stations. The second

option was preferred, both for the Class 156 retrofit and for the AT200 units. In the case of the Class 156 it was found that (on a per vehicle basis) the use of a 250kW traction motor would require a fuel cell of approximately 200kW power rating, together with a battery pack of about 20kWh storage capacity and 200kW power rating. Hydrogen storage tanks would be pressurised to 350 bar (approximately 5000 lb/sq.inch), as in many other transport applications. The gas storage capacity per vehicle for a 500-mile operating range on the route considered in the study (in East Anglia) was at least 63kg [16]. Removal of all existing equipment between the bogies of each coach was found necessary to allow for the storage tanks and hardware for the hybrid powertrain and this would mean a reduction in gross weight of about 5 tonnes in the case of the Class 156. About 2000 kg of hydrogen would be required per day for a fleet of 25 modified Class 156 units. However, allowing for costs of the vehicles and the installation of the hydrogen production plant, the payback period would be about twenty years. This is not particularly attractive but, taking the South Wales valley lines as an example, the investment for a fleet of 25 units was about one seventh of the estimated cost of conventional electrification [16]. For hydrogen obtained from reforming, the reduction in overall emissions would be 43% compared with the unmodified diesel unit with fuel costs per mile estimated to be 63% less. However, if grid-powered electrolysis was used (with the 2016 mix of generation methods) the carbon emissions were estimated to be 33% greater than with diesel power [16]. Although important questions of cost remain to be answered, electrolysis from renewable sources (giving zero emissions) has advantages, especially when the continuing reductions in the cost of electricity from renewables is taken into account.

One example of hydrogen-powered trains in passenger service is in Lower Saxony in Germany where Alstom hybrid *Coradia iLint* two-coach multiple units operate on a 50 km route. These 98 tonne trains have a maximum speed of 140 km/hr and allegedly show lower operating costs than the equivalent diesel units that they replaced. A full tank of hydrogen provides a range of about 1,000 km [17]. Vivarail is actively developing a hydrogen powered train, involving a hydrogen/battery-electric version of the company's diesel/battery-electric Class 230 [18]. In the hydrogen powered version of the Class 230 the fuel cell and storage tanks would be located below the floor in the intermediate vehicle of a three-car sets. The unit would have a range of 650 miles and would incorporate regenerative braking. A modular design approach has been adopted in the Vivarail Class 230 units, allowing a straightforward transition from a diesel/battery to a hydrogen/battery hybrid configuration.

Other projects announced recently in the UK include the Porterbrook/University of Birmingham *HydroFLEX* demonstration project based on a Class 319 unit [19]. A hydrogen-powered train for the UK market is also under development by Alstom and Eversholt Rail. Known as the *Breeze*, this will be based upon an existing Class 321 multiple unit [20]. Elsewhere in Europe, an order for hydrogen fuel cell powered electric multiple units has been placed with Stadler by the Zillertalbahn in Austria. This is for five train sets to operate on the 760mm gauge 31.7 km long route from Jenbach to Mayrhofen. Hydrogen will be provided using electricity from local hydro-electric supplies [21]

Even superficial comparisons of battery power and fuel cells suggest that the latter have an advantage in terms of range but respond sluggishly to a demanded increase in power output. The real benefits of fuel cells may only be achieved, with current technology, when used within a hybrid system involving other elements such as batteries or other types of storage device. These allow regenerative braking and also provide additional power when required, such as at the start and during the acceleration phase. However, such hybrid systems inevitably involve additional cost and added complexity.

Locomotive-hauled trains provide an interesting alternative to multiple units because the locomotives could also be used for freight. A study of a 601km non-electrified section of the Trondheim to Bødo route in Norway concluded that a locomotive with hydrogen fuel cells within a hybrid powertrain would have advantages over a purely battery-powered equivalent and over a period of twenty years, both options were found to give lower overall cost estimates than conventional electrification [22], [23].

Although hydrogen fuel cells have a potentially important role in rail transport, a report from the Institution of Mechanical Engineers in 2019 pointed out that, with present-day costs, hydrogen production based on electrolysis is almost three times more costly than electricity for traction on a conventional electrified railway [24]. That report suggests that hydrogen power is best used in areas where hydrogen is available from renewable sources. This is especially attractive in situations where there may be, at times, a surplus of renewable energy, due for example to limited capacity in the transmission and distribution systems. An important indication of the potential importance of hydrogen power in Scotland is a recently announced initiative, supported by Scottish Enterprise, to modify a Class 314 three-coach electric multiple unit to form a test-bed for hydrogen fuel-cell and battery power. The unit was donated for the project by ScotRail and the conversion is to be carried out by Brodie Engineering Ltd at Kilmarnock. It is intended that testing of this vehicle should be carried out in Scotland [6].

1.3 Regenerative braking in battery-electric and hybrid rail vehicles

Regenerative systems, in which the traction motors supply energy back to the distribution grid during braking, are well-established on conventional electrified railways. On-board systems for regenerative braking on non-electrified routes can also be useful for battery-powered vehicles or on vehicles equipped using another form of electrical storage device known as a "supercapacitor" or "ultracapacitor". These have a much higher specific power (kW/kg) than batteries but lower specific energy density (kWh/kg) and are therefore capable of absorbing large amounts of energy during braking, storing it for a short time and then returning it to the traction motors during subsequent periods of acceleration [25]. In Europe, practical rail applications of supercapacitors began in 2003 with tests in Germany of a prototype light-rail vehicle from Bombardier. A power level of 600kW was available in starting and the vehicle could move independently for about one kilometre, producing a saving, allegedly, of up to 30% of total energy costs. In August 2012 the CSR Zhuzhou Electric Locomotive Corporation of China announced that it was developing a prototype two-car light metro train with a supercapacitor unit. This train could travel up to 2 km using only energy stored in the onboard supercapacitors and the system could be recharged in 30 seconds at stations via a ground mounted pickup [26]. One interesting possibility involves hybrid systems equipped with fuel-cells, batteries and supercapacitors so that the high specific energy density of batteries is combined with the high specific power and longer life of supercapacitors [27].

1.4 Objectives of the work

It is believed that mathematical modelling and simulation methods can provide valuable insight concerning issues arising in the design and optimisation of powertrain systems. The main objective in the preliminary work being reported here is to use a standard train performance model and appropriate computer simulation techniques to examine the effects on the performance of a hybrid multiple unit of the power ratings of the traction motors, hydrogen fuel cell and battery, along with the battery storage capacity. These power ratings are of critical importance and the energy stored in the battery must be sufficient at each point on the route to allow the schedule to be maintained over the next stage of the journey. Battery life is another significant factor in the design of a vehicle of this kind and the pattern of charging and discharging while in service, which depends on overall energy management and control, is important. Design choices made in terms of the traction motors, battery, fuel cell and hydrogen storage tanks have a direct effect on the train weight which, in turn influences performance. Therefore, as in most other engineering design situations, the process is an iterative one and can never be viewed as having a unique solution.

The timescales currently being required by governments are demanding and it is important that designs offer maximum flexibility and optimum performance. This work puts particular emphasis on the design of the train, but it has to be recognised that there are other important aspects such as the provision of

hydrogen supplies and the design of re-fuelling systems. Such issues are not discussed in this report as they have been considered in detail elsewhere (e.g. [16] and [24]).

This report builds on two earlier reports prepared by the author for the Scottish Association for Public Transport in 2019 [28], [29] and also on a technical paper by the author on the application of inverse simulation methods to train performance problems which was published in the Proceedings of the Institution of Mechanical Engineers in 2017 [30].

2. The train performance model

The mathematical basis for train perfomance system modelling is well established. Train performance models are based, conventionally, on a set of ordinary differential and algebraic equations representing the characteristics of the traction system and vehicles. Information about the route is also an essential part of the complete simulation model. These models are nonlinear in form and analytical methods of solution are therefore inappropriate, except in special cases. Numerical methods of solution are needed, using a computer-based approach. Comparisons of simulation model results with measured data from practical train performance tests for equivalent conditions have demonstrated, previously, the validity of this approach (see e.g. [31], [32]).

In lumped-parameter mathematical models conventionally used for train-performance investigations, the distance travelled as a function of time, $x(t)$, is considered as one of the output quantities, along with the velocity $\dot{x}(t)$ and the acceleration $\ddot{x}(t)$. In the simplest case the train is regarded as a single mass acted upon by the tractive force, braking force, a gravitational force associated with gradients and forces representing other components of the resistance to motion. From the application of Newton's Second Law the equation of motion has the form:

$$M\ddot{x}(t) = F_T(t) - F_B(t) - R(t) \pm Mg\sin\alpha(x(t)) \tag{1}$$

where $F_T(t)$ and $F_B(t)$ are the tractive force and braking force. The variable $R(t)$ is the resistance to motion, g is the acceleration due to gravity, α is the gradient angle of the track which is depends on the train position $x(t)$ and M is the mass of the train which is regarded as constant.

The resistance $R(t)$ in equation (1) involves three constants, A, B and C which are known as the Davis coefficients. Values of these coefficients are based on empirical estimates for the specific vehicles being considered, giving an overall expression for resistance of the form:

$$R(t) = A + B\dot{x}(t) + C\dot{x}(t)^2 \tag{2}$$

where A and B depend on the mass M and the coefficient C depends on aerodynamic factors. It should be noted that although this model does not include resistance due to curves this may be incorporated through an additional resistance term that depends the on the location of the train.

It should also be noted that the terms F_T and F_B in (1) are such that at all times when the tractive force term F_T has a non-zero value the braking force F_B is zero. Correspondingly, when the braking force F_B has a non-zero value the applied tractive force F_T is zero. Hence, within the simulation, these terms can be taken together to form a composite tractive force variable $T(t)$ which can be positive or negative.

The power $P(t)$ is then given by the equation:

$$P(t) = T(t)\dot{x}(t) \tag{3}$$

This shows that, for a specific level of power, the available tractive force falls as the velocity $\dot{x(t)}$ increases. It is assumed that for speeds below a specific value, V_{ch}, the available tractive force is limited to a value $\pm T_0$ to ensure that adhesion between the driven wheels and the rails is maintained, even under adverse environmental conditions.

The energy consumption E over the period from the start $t = 0$ to time $t = \tau$ is given by:

$$E = \int_0^{\tau} P dt \tag{4}$$

In general, braking action in trains may be frictional or may involve regeneration. Regenerative braking strategies usually involve a blend of frictional and electrical braking. With purely frictional braking it may be assumed that the driver applies a progressive braking strategy in which the braking force has, more or less, an inverse relationship with speed. The braking power is considered constant in the first phase of braking and, in the model used here, this is equal to the maximum power available at the wheels. In the second phase of a frictional braking strategy, the braking force may be taken as equal to the tractive force value at the adhesion limit, T_0. When regenerative braking is used, as in the proposed hybrid multiple unit, the braking force is assumed to be limited by the power rating of the traction motor, electronic components and battery and is inversely proportional to the speed. As the speed falls, the braking force therefore increases. When the speed drops to the value at which the braking force is at the adhesion limit, T_0, resistive braking is applied (usually manually) using that limiting value of braking force until the train comes to rest. Application of these blended regenerative and frictional braking strategies gives a maximum rate of change of speed during braking which is similar, but opposite in sign, to the maximum acceleration of the train. At the instant when the speed reaches zero the thrust, resistance and gradient terms in the equation of motion are all switched to zero to ensure that no further movement can occur.

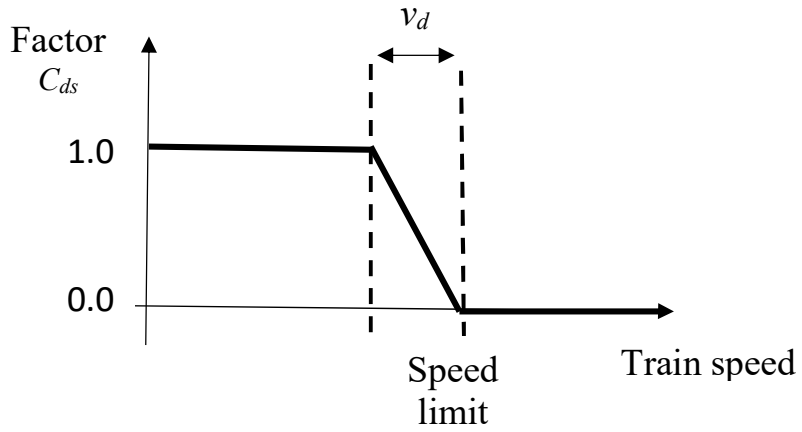

Figure 1. Diagram illustrating driver action in the train simulation model to take account of speed limits.

Train performance simulation models must include speed restrictions and a feature has been included in the computer simulation models used in this investigation to allow for transitions to speed-limited sections of route. This is represented by a simplified model of driver action in which speed is compared continuously with the defined speed limit for the point on the route at which the train is operating. A time-varying factor $C_{ds}(t)$ is introduced and, if the speed is above the limit, this factor is set to zero, while if the speed is below the limit by an amount v_d (or more), the factor $C_{ds}(t)$ is given a value of unity. Between these critical speed values $C_{ds}(t)$ varies with train speed between 0 and 1 in a linear fashion, as shown in Figure 2. The tractive force value at each time step in the simulation is multiplied by the factor $C_{ds}(t)$ to represent driver control actions in approaching and adhering to the speed limit. The tractive force thus changs from the steady value used just before the speed limit, through a steadily falling range of values as the limit is approached, to a value of zero when the speed becomes equal to or greater than the limiting value. A parameter v_d, is used to define the speed difference at which driver action is initiated when approaching a speed limit. This has been chosen to be 1 ms^{-1} (3.6 km/hour) for this example as the only speed restriction for the chosen test route is an overall line speed limit. Other

numerical values for v_d might be more appropriate for other forms of speed restriction and different methods for representing driver control action could be considered. However, the method outlined was thought to be an appropriate, simple and easily-implemented approach. Braking action could be introduced during the approach to a speed restriction by using a method similar to that outlined above for implementation of the braking phase.

Figure 2 is a block diagram of the chosen form of hybrid powertrain system with fuel cells and battery coupled to a traction motor through dc/dc converters and an inverter. It should be noted that this diagram includes the additional load associated with auxiliaries, such as heating and air-conditioning. For simplicity, it has been assumed that this is supplied by the fuel cell at all times. The fuel cell electrical output available for traction or for recharging the battery is therefore reduced by a constant amount equal to the average power required for auxiliary services. It should also be noted that the dc/dc power electronic converters connected to the battery are bi-directional, as is the dc/ac inverter. However, the dc/dc converter associated with the fuel cell is unidirectional as the fuel cell cannot absorb energy.

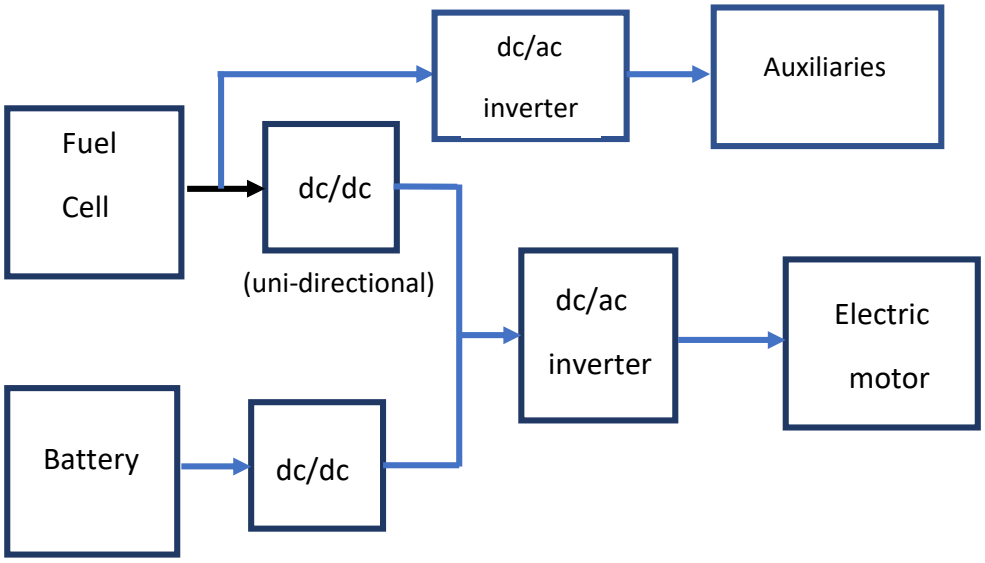

Figure 2: Block diagram of a hybrid system with fuel cell and battery coupled to a traction motor through dc/dc converters and an inverter.

The overall form of the train performance model used for the simulation studies involving the hybrid fuel-cell/battery electric units is based on equations (1) to (4) and includes the hybrid powertrain components of Figure 2. The fuel cell is the primary source of energy. and when its output is not fully required for traction (e.g. during cruise conditions on level track, or when the train is coasting or stationary) the fuel-cell is used to charge the battery. The battery is thus used, primarily, to provide for transient changes in power demand from the traction motors and to provide additional tractive force on rising gradients. In addition, energy produced by regeneration during braking provides an important contribution to battery charging.

The fuel cell model involves an ideal energy source with a specified output power rating. It is the main element of the powertrain in which dynamic effects could be significant in relation to the overall dynamics of the train since fuel cells can take a significant time to respond to a demanded change in output power level. However, a more complex representation of the fuel cell was not considered necessary since it has been assumed that the fuel cell operates, mainly, in a condition close to an optimum steady-state condition chosen to maximise efficiency. The battery is also represented by a highly simplified model, but allowance is made for the energy loss within the battery between charging and discharge, which introduces an effective efficiency factor for the battery. No dynamic effects are

included, and the power electronic components of Figure 2 also involve simplified representations in which dynamic behaviour is again neglected. The output power of each inverter or dc/dc converter is taken to be a fixed percentage of the input power (for power transfer in both directions in the case of the bi-directional units). Similarly, a highly simplified form of model is used to represent the traction motors, with the power at the rail being a fixed percentage of the inverter power level.

The powertrain sub-model used includes only a very simple form of energy management or control system. In this scheme the fuel cell provides a constant power output at most times. If the power demanded at the rail is less than the power output available from the fuel cell (allowing for losses in the power electronic converters and traction motors) the rest of the fuel cell output is used to charge the battery. During braking the power required at the rail reverses in sign in the simulation model and the required braking force is provided using a blended combination of regerative and frictional components. During the first phase of the blended braking strategy regenerative braking is used (in part) and 50% of the power from regeneration is assumed available for battery charging. During that phase the power output from the fuel cell is reduced to an idle level involving only the constant component which supplies the auxiliaries. Regenerative braking is used until the train speed drops to the value at which tractive effort limiting occurs. From that time, until the train comes to rest (or until positive power is applied again), a constant braking force is applied (equal in value to the tractive force adhesion limit T_0) and this braking action involves use of the conventional frictional brakes only. During regeneration, the efficiency of the traction motors (acting as generators) is taken, for the purposes of the model, to be the same as the efficiency in normal operation.

3. Route characteristics

Before considering how batteries, fuel-cells and other powertrain elements could meet the future needs of routes in Scotland, we must consider the nature of some the lines involved. The distances are considerable compared with other routes where alternative energy sources have been considered. For example, the total journey from Glasgow Queen Street to Oban is about 101 ½ miles (approximately 160 km), to Fort William 123 miles (217 km) and to Mallaig 165 miles (264 km). The start of these routes is close to sea level, as are the destinations. However, the summit of the Fort William line is 1347 ft (about 415 m) above sea level and in both directions there are many prolonged stretches where trains experience continuous gradients of 1 in 60 for several miles, combined with many sharp curves and local speed restrictions. Journey times between stations for the West Highland line, as shown in the current ScotRail working timetable, vary from 5½ minutes to 20 minutes with an average of just over 12½ minutes. The average distance between stations is about 8 miles (just over13 km).

Rather than use route information for a specific railway line, a special test route has been created for this preliminary simulation study. It includes elements that are considered typical of lines on which hybrid hydrogen fuel cell and battery electric multiple units might be used. The length of the test route has been chosen to be approximately 15 km. It involves five distinct phases of operation – a) the initial acceleration to the maximum allowed speed, b) a steady-state phase involving a spell of continuous operation at that line-speed limit, but with a significant change of gradient en route, c) a further section of level track, d) a coasting phase and e) a final braking phase to bring the train to rest. In the example being considered the coasting phase begins at a distance x_C from the start (chosen as just over 12¼ km in the cases considered here) and the braking phase at a distance x_B (about 13¼ km). The chosen gradient profile is shown in Figure 3 and involves level track for an initial distance of 4 km and then a constant rising gradient of 1 in Y for 4 km. This gradient, expressed as a percentage, is $100/Y$ % and the angle α in equation (1) is related to Y through the equation:

$$\sin\alpha = 1/Y \tag{5}$$

The value of Y chosen initially for the test route gives a gradient of 1 in 50. For simplicity, additional resistance on curved track has been neglected. There is an overall line speed restriction in terms of a line-speed limit of 96km/h (60mph).

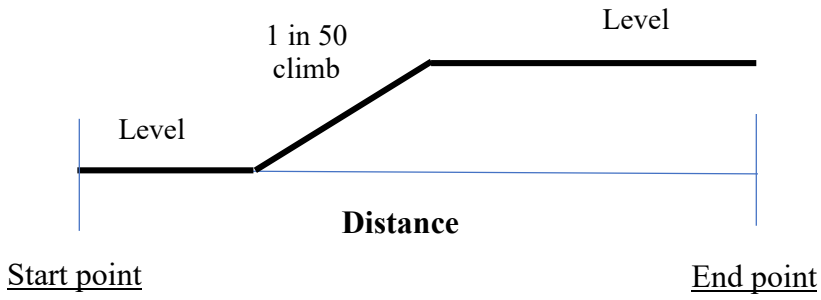

Figure 3: Gradient profile of route considered in the simulation studies.

4. Simulation methods

4.1 Conventional forward simulation techniques and tools

Simulation techniques allow experiments to be carried out on mathematical models and the extent to which results from a simulation study can be taken as being an accurate representation of equivalent results from the real system depend on a wide range of factors. Assumptions and simplifications made in developing the underlying logical and mathematical description are of key importance and much has been written about the testing and validation of simulation models (see, for example, [33], [34]).

Computational tools for the simulation of systems that can be described mathematically by sets of ordinary differential equations and algebraic equations are of particular importance for studies of train performance. There are many widely-available continuous system simulation software packages that are suitable for this type of investigation. Such tools allow the user to concentrate on the problem in hand and thus avoid having to deal with underlying issues of numerical methods and the associated programming tasks. They use well-proven numerical techniques and are usually well-documented, thus offering significant benefits in terms of robustness and transparenc. This applies both to the simulation aspects of the work and to the associated tasks involving data manipulation. Examples of widely-used simulation tools include the commercially-supported MATLAB® software [35] and its associated Simulink® graphical environment, and the broadly-similar open-source Scilab software [36].

The simulation programs developed for this work were written in MATLAB® code using standard MATLAB® '*ode*' routines for solution of the ordinary differential equations that are central to the train performance model presented in Section 2. Several different *ode* routines are available within MATLAB® but the all results presented here are based on the use of the low-order *ode23* routine which involves a Runge-Kutta type of algorithm. Compared with some other available MATLAB® routines, this has relatively low accuracy but has advantages in terms of speed of solution.

4.2 The inverse simulation approach

Computer simulation methods used for train performance investigations conventionally apply tractive force or power as input variables. However, in the work described in this report use is also made of models which work in reverse through an inverse simulation approach. As shown in Figure 4, the input to the conventional simulation model could be power or tractive force, with distance travelled, speed or acceleration as typical outputs. In the inverse simulation model the input could be a desired time history in terms of distance travelled or speed versus time, while the outputs might be the time history of tractive force, power or energy needed to achieve that schedule.

For train performance studies conventional simulation may provide the user with a distance-time record for a given route, allowing for constraints on speed in terms of the overall speed limit and local speed restrictions. Inverse simulation can be used to investigate the effects of variations of design features

(such as train mass or resistance parameters) on the energy requirements in meeting a given schedule, or to investigate power and energy implications of reducing or increasing the journey time. Benefits of the inverse simulation approach claimed in other areas of engineering, such as helicopter flight control (see, for example, [37]), include more design insight and, espccially, more direct investigation of design trade-offs than may be possible through the use of conventional forward simulation alone. Examples of this use of inverse simulation in train performance investigations may be found in earlier work reported in [30].

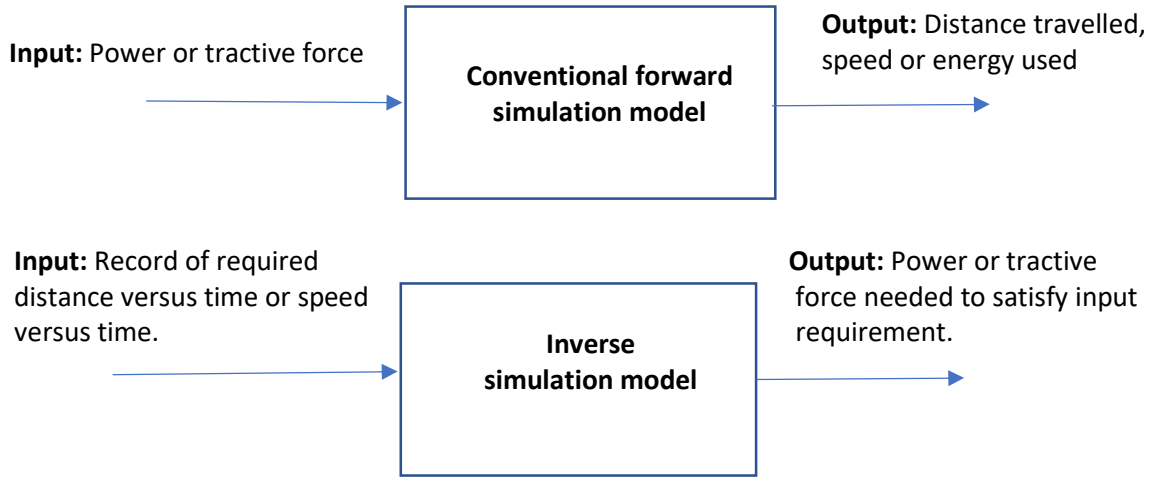

Figure 4: Block diagrams showing comparison of conventional forward simulation and inverse simulation approaches for train performance studies

Many different methods have been developed for inverse simulation (see e.g. [38], [39] and [40]) and these can be implemented using standard simulation tools such as MATLAB®. The specific method of inverse inverse simulation used in the work presented in this report has been described in detail elsewhere (e.g.[30], [41] and [42]) and involves the application of a high-gain feedback path around a conventional forward train performance simulation model (as described in more detail in Section 5.1.2)

5. Simulation results

The first task in carrying out simulation-based investigations of possible configurations for fuel-cell/battery electric hybrid trains involves creating appropriate reference input data. One approach is to use a simulation of an existing type of train on the test route described in Section 3. The type of train considered here is the Class 156 two-car diesel multiple unit (dmu) and this was chosen because it is currently used on routes such as the West Highland lines from Glasgow to Oban, Fort William and Mallaig and, in the south of Scotland, on services from Glasgow to Stranraer. Another reason for including this type of unit in the study is that it was one of two types of vehicle discussed in the 2016 FCEMU report mentioned in Section 1 [16]. Parameter values used for the Class 156 simulation model are given in Table A1 in the Appendix, where simulation results for a Class 156 unit are also presented for the test route being considered.

The information in the Appendix shows that, for a two-coach Class 156 dmu, the maximum power at the rail is 348.48 kW with the model showing that the power required to maintain the steady 96 km/h speed is approximately 175 kW on level track. Along with data from the 2016 FCEMU report [16], these values for the Class 156 performance were a starting point in considering the specification for a hybrid fuel-cell/ battery electric unit to provide equivalent performance. Table 1 shows the set of parameters used in the first set of simulation runs. From those parameter values the maximum power at the rail for the 2-coach hybrid unit involves 251.7 kW from the fuel cell and 180.6 kW from the battery,

giving a total of 432.3 kW. This is greater than the power available at the rail in the Class 156 unit and the decision to use these initial values and thus provide additional power made allowance for possible journey-time reductions. The performance is highly dependent on weight which is affected particularly by the number of battery units needed which is, in turn, determined by the required energy storage capacity. Using weight analysis information provided by Kent and his collaborators [16], the weight of a fuel cell module is approximately 5kg per kW and the weight of a battery pack 23 kg/kWh.

Table 1: Parameter values used in initial simulation runs for the two-coach hybrid fuel-cell and battery-electric unit.

Quantity	Symbol	Numerical value with units
Traction motor power rating	P_M	2×200=400 kW
Hydrogen fuel cell power rating	P_F	300 kW
Battery power rating	P_B	250 kW
Train mass (gross)	M	90,000 kg (90 tonnes)
Tractive force at zero speed	T_0	50 kN
Traction motor efficiency	η_M	0.95
DC/DC converter efficiencies	η_{DC}	0.975
Inverter efficiencies	η_{INV}	0.975
Battery efficiency	η_B	0.85
First resistance coefficient	a	1500 N
Second resistance coefficient.	b	6.0 $Nm^{-1}s$
Third resistance coefficient	c	6.7 $Nm^{-2}s^2$
Gravitational constant	g	9.81 ms^{-2}
Power for auxiliaries	P_A	40 kW

Table 1 does not include the maximum battery storage capacity as this parameter is of central importance in terms of this investigation. The value suggested in the 2016 FCEMU report by Kent et al. [16] is at least 20 kWh per vehicle, but battery pack sizing in that study was done mainly on the basis of the energy to be absorbed if the train were braking from the maximum operating speed. The battery would then provide addditional energy during the subsequent acceleration. However, the project described in this report puts much more emphasis on the use of battery power for longer periods of time, especially where the train is ascending steep inclines as well as during periods when the train is accelerating. On downhill sections when the train is coasting or operating at less than full power the battery would receive charge from the fuel-cell, as would happen also during periods of braking and when the train is at rest. It is likely, therefore, that the total battery storage capcity of a two-coach hybrid multiple unit would have to be significantly greater than the figure of 40 kWh proposed for the application considered by Kent and his colleagues [16]. This design strategy is consistent also with what is known about the Alstom Coradia *iLint* units operating in Germany, although limited technical information appears to be available publicly about these trains.

The state of charge of the battery is of particular interest since it is important that the battery charge should never fall too low and there must always be sufficient charge at each stage of the journey to ensure that the train can maintain its schedule using a combination of battery power and power from the fuel cell. The effect of having too little installed battery storage capacity is that transient demands on the fuel-cell would increase since there could be times when stored battery energy would not satisfy the demand. This would mean that the fuel cell could not operate in a steady state condition at, or close to, the optimum operating point at all times and the sluggish response of the fuel cell to demanded changes of power output could also become an issue.

Getting the right balance between fuel cell power output, the maximum battery power level and battery storage capacity involves difficult design decisions, even without taking account of the important and directly related issues of the weight and volume of fuel cells, batteries and hydrogen storage tanks and the asssociated costs of these components. The initial value of battery stored energy in each of the simulation results of Section 5 is 100 kWh and some of those results show stored energy values in excess of that figure. However, this should not be taken to suggest that more than 100 kWh of battery storage capacity should be provided, since allowing for more stored energy introduces significant weight penalties.

The effects of varying the power ratings of the fuel cell and battery are clearly of critical importance in terms of the performance of the hybrid unit. Other parameters of the train model, such as the mass, traction motor ratings and the Davis resistance coefficients, also have an important bearing on performance and their effects can be investigated very easily through simulation. All of the simulation results in Sections 5.1 and 5.2, taken together, should allow the initially chosen parameter values shown in Table 1 to be reviewed and a realistic figure to be found for the minimum battery storage capacity required.

5.1 Simulation results for a hybrid two-car fuel-cell/battery-electric multiple unit

5.1.1 Forward simulation results

Simulation results for the two-coach hybrid fuel-cell simulation model for the test route described in Section 3 and the parameter values given in Table 1 are shown in Figures 5 – 10, with Figures 5 and 6 showing the speed versus time and distance versus time records, respectively. The total distance travelled is 14.92 km and the travel time is 679 s. It should be noted that the distance versus time plot of Figure 6 is similar to the straight line type of plot traditionally used to represent train schedules, where the slope represents the average speed between two stations. However, in Figure 6, the subtle variations of the gradient are very signifcant and reflect the much sharper changes seen in the speed versus time plot of Figure 5 and the tractive force record of Figure 7.

The tractive force time history is influenced, very strongly, by the nature of the route involved, as is the speed versus time record of Figure 5. During the initial acceleration the tractive effort is limited by adhesion constraints to 50 kN before reaching the constant power condition at a speed of 8 m/s (about 29 km/h). For values of speed greater than this value the tractive effort falls as the speed increases. When the speed reaches the line limit of 96 km/h the power at the rail (Figure 8) falls to below half of the maximum used during the initial accceleration. The start of the 1 in 50 rising gradient brings the power level back to the maximum available, with the tractive force increasing as the speed drops. The level track beyond the summit allows the train to accelerate again at full power until the line speed limit is reached once again. Coasting starts at 12 km and regenerative braking is applied at 14.3.km. In the final stage, when speed has fallen below 8 m/s, frictional braking is used with a negative tractive force equal to the 50 kN adhesion limit. When regenerative braking stops the battery is charged from the fuel cell through the dc/dc converters at a rate corresponding to the maximum power rating of the battery.

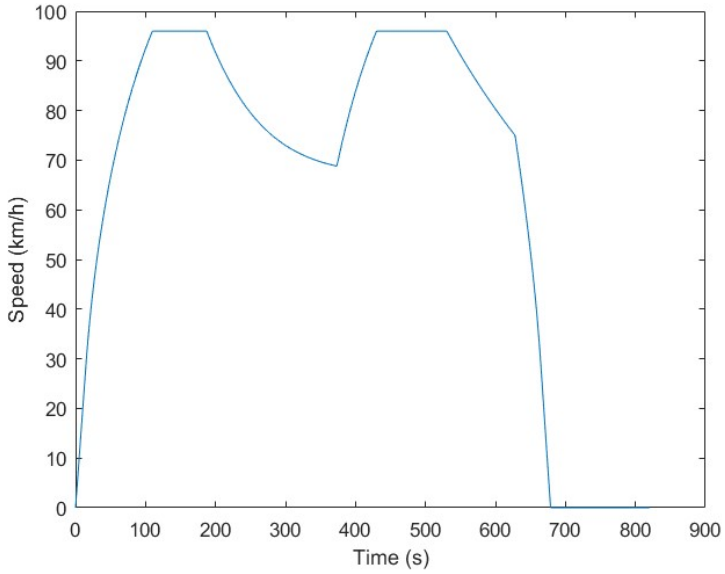

Figure 5: Forward simulation results showing a record of speed versus time for the two-coach hybrid unit on the test route for the parameter values of Table 1**.**

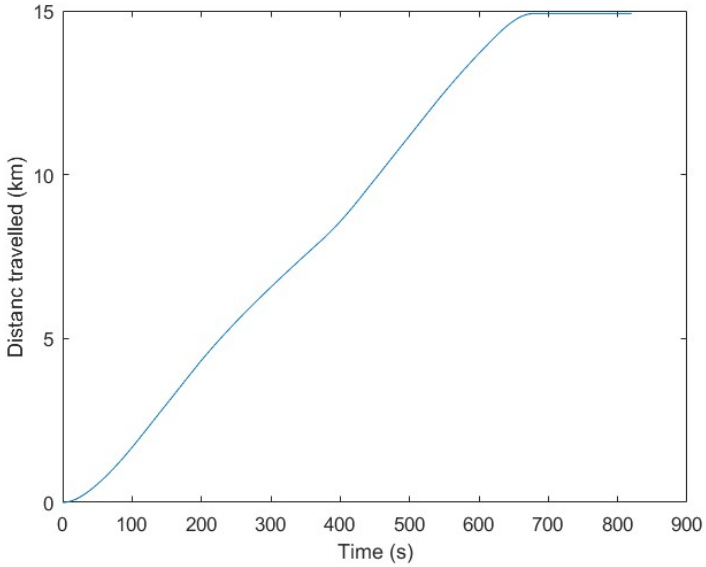

Figure 6: Forward simulation results showing a record of distance travelled versus time for the two-coach hybrid unit on the test route for the parameter values in Table 1**.**

The record of power at the rail in Figure 8 includes the component from the fuel cell (constant except during regenerative braking) and an additional component involving the battery. In Figures 7 and 8 negative values represent braking actions, both through regenerative braking and frictional braking.

Figure 9 shows the power at the battery terminals and, in this case, negative values of power show that the battery is supplying energy to the traction motors while positive values indicate that the battery is charging. The large power demands on the battery during the initial acceleration and during the ascent of the 1 in 50 gradient are clearly seen. During the period when the train is running at the line speed limit of 96 km/h there is enough power available from the fuel cell to allow some charging of the battery. When coasting, the power at the rail drops to zero and the fuel cell ouput (apart from the component supplying the auxiliaries) is used to charge the battery. Charging continues in the early stage of braking, with one half of the total braking power being assumed available for charging. This is consistent with assumptions made in previous studies involving regenerative braking and the effect can be seen in Figure 9 where a slight drop in the battery charging power level occurs between about 610 s and 640 s.

Once frictional braking takes over the fuel cell is used once again for battery charging and charging also takes place when the train is at rest.

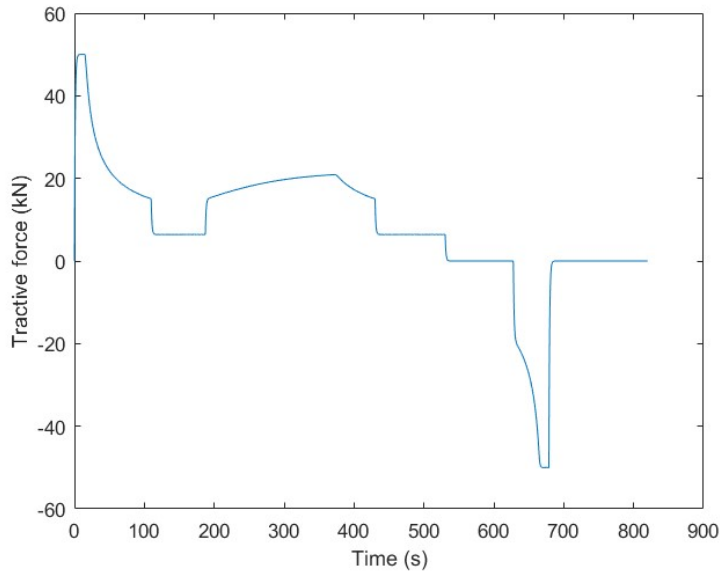

Figure 7: Forward simulation results showing a record of tractive force versus time for the two-coach hybrid unit on the test route for the parameter values in Table 1**.**

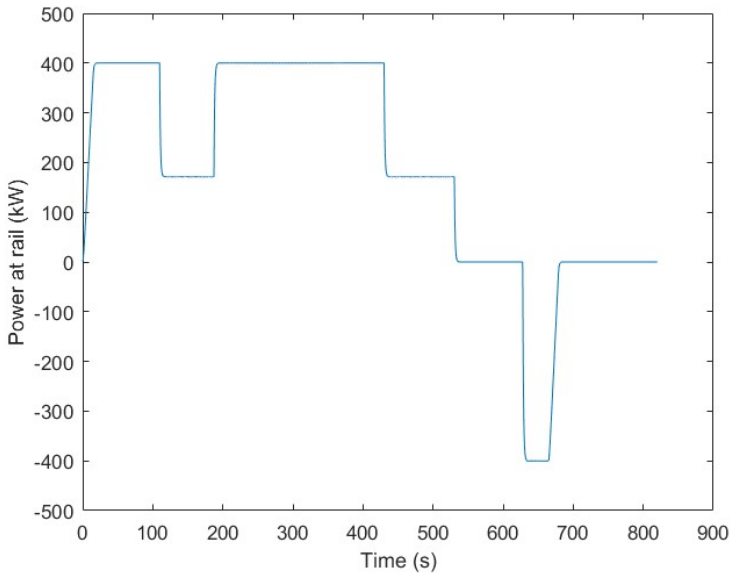

Figure 8: Forward simulation results showing a record of power at the rail versus time for the two-coach hybrid unit on the test route for the parameter values in Table 1**.**

Figure 10 provides information about the stored energy within the battery. During most of the acceleration phase there is a steady reduction in stored energy. This results from the need for energy from the battery to be used to supplement the output from the fuel cell. During the short phase where the train is running at the line speed limit on level track the stored energy increases, but once the train is on the section of the route with the rising gradient the stored energy falls at a rate of more than 3 kWh/minute. When the train is running on level track again, at the line speed limit, the battery starts to re-charge. During the brake application the battery continues to be charged, either from the traction motors acting as generators or directly from the hydrogen fuel-cell. The rate of charge when the train is at rest is about 3.5 kWh/minute. This record of energy stored in the battery is consistent with the pattern of battery power in Figure 9. It is assumed that during the regenerative braking phase the fuel

cell supplies only the auxiliary load. The battery is then being charged using only the electrical output supplied by the traction motors through the inverter and reversible dc/dc converter.

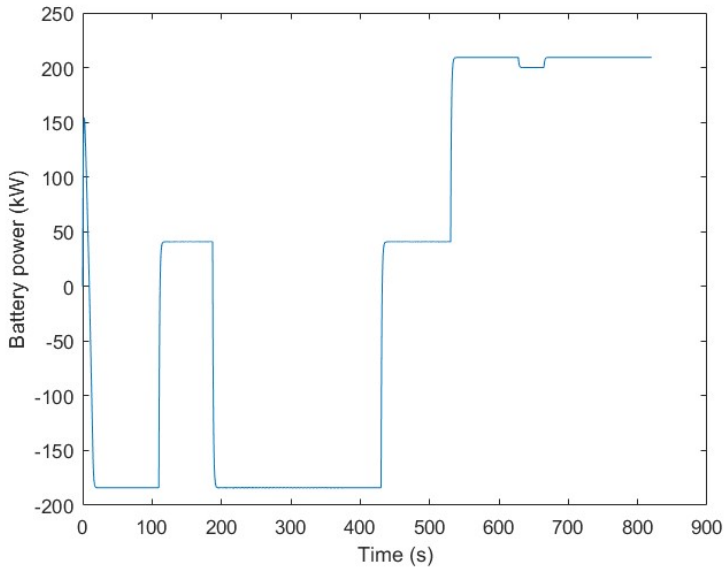

Figure 9: Forward simulation result showing a record of battery power versus time for the two-coach hybrid unit on the test route for the parameter values in Table 1**.**

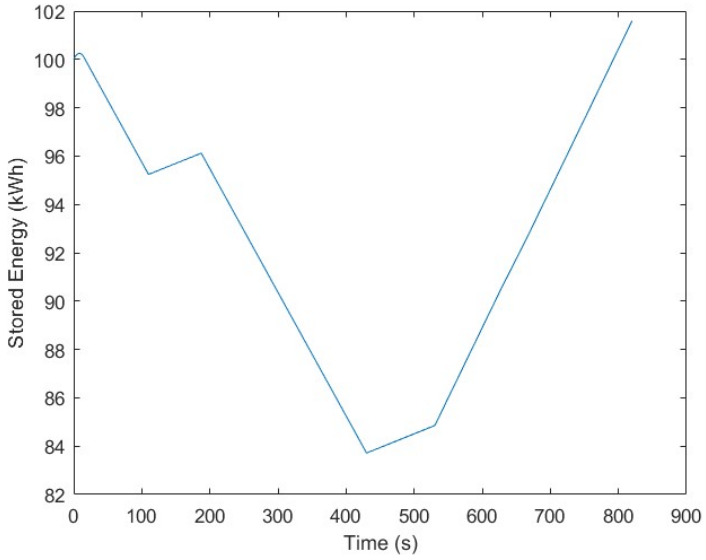

Figure 10: Forward simulation results showing a record of battery energy versus time for the two-coach hybrid unit on the test route for the parameter values in Table 1**.**

One interesting feature of the simulation results in Figure 10 (for the fuel cells with the 300 kW power rating) is that the battery is being charged during the periods when the train is running at the line limit of 96 km/h. This suggests that the size of fuel cell could possibly be reduced or that this hybrid multiple unit could be used on routes with a line speed limit greater than the 96 km/h considered here. However, the results also show that the stored energy in the battery when the train comes to rest (about about 680 s after the start) is below the initial level of 100 kWh. However, it can be seen that after a further 90 s of charging at rest, which is typical of a station dwell time on the routes being considered, the stored energy level has risen to a value very close to that at the start.

Simulation results are shown in Figures 11 – 13 are for cases involving other fuel-cell power output levels. A change of fuel cell power output from 300 kW to 350 kW, with other parameters kept at the

values in Table 1, has the effects shown in Figures 11 and 12. There is no change in total power used and the only change is the power available for charging the battery. Thus the pattern of battery power versus time in Figure 12 and the reccord of energy stored in the battery in Figure 11 are different from the previous results, although the journey time, distance travelled and power at the rail remain as before. As would be expected, the power from the battery has fallen to compensate for the increase in the power available from the fuel cell and the stored energy in the battery is therefore depleted to a smaller extent. Figure 11 shows that, at the minimum, the stored energy has fallen by about 10 kWh compared with the value of about 15 kWh in the previous case shown in Figure 10. This means that the stored battery energy falls at only 2.1 kWh/min during the initial acceleration and on the gradient section.

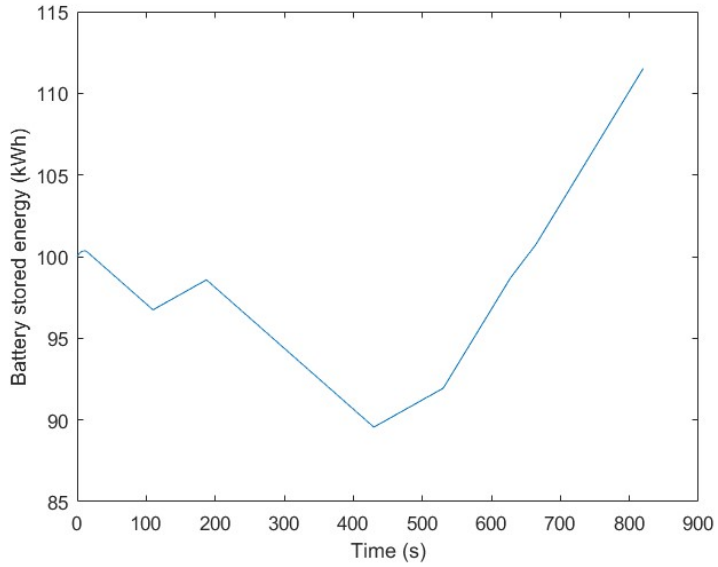

Figure 11: Forward simulation results showing a record of battery energy versus time for the two-coach hybrid unit on the test route for the nominal parameter values in Table 1 but with the fuel-cell power rating increased from 300 kW to 350 kW**.**

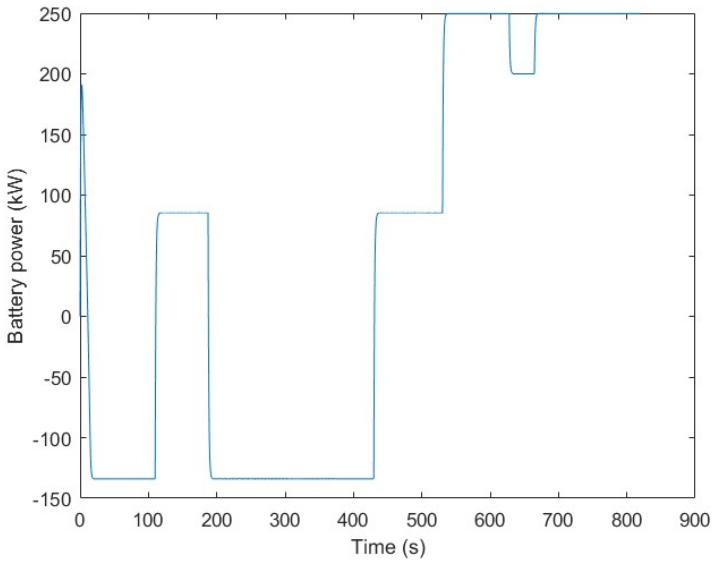

Figure 12: Simulation results showing a record of battery power versus time for the two-coach hybrid unit on the test route for the nominal set of parameters of Table 1 but with the fuel-cell pwer rating increased from 300 kW to 350 kW.

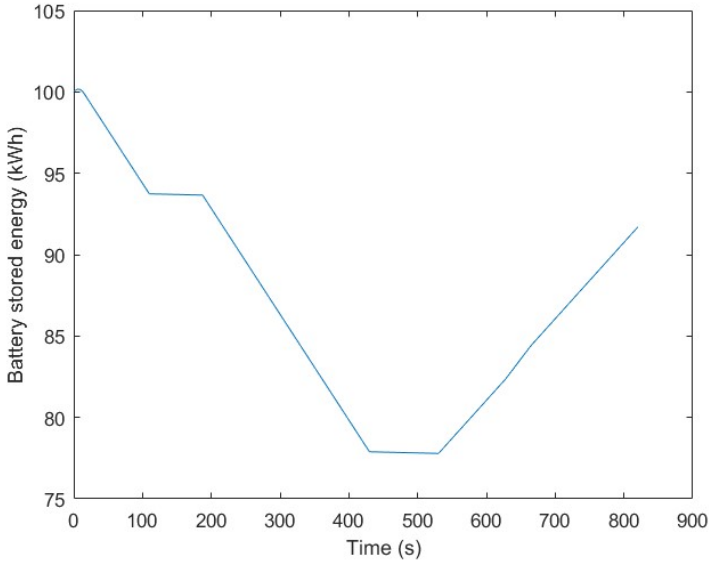

Figure 13: Simulation results showing a record of battery energy versus time for the two-coach hybrid unit on the test route for the nominal set of parameters of Table 1 but with the fuel-cell pwer rating reduced from 300 kW to 250 kW**.**

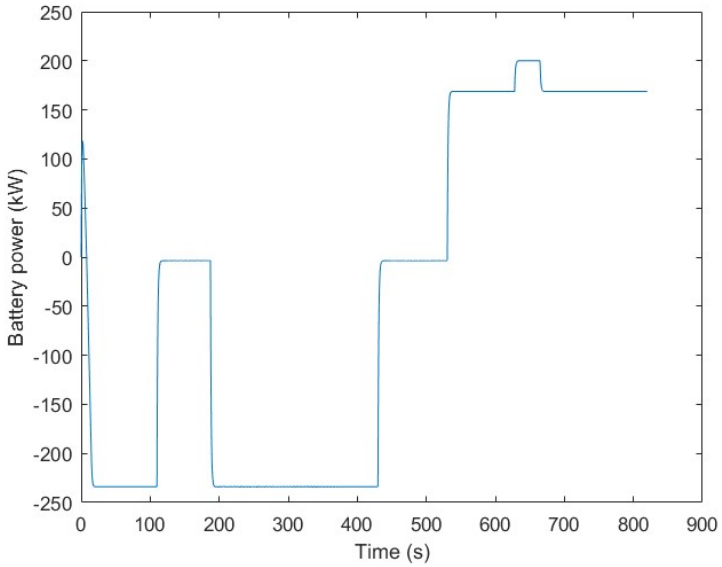

Figure 14: Simulation results showing a record of battery power versus time for the two-coach hybrid unit on the test route for the nominal set of parameters of Table 1 but with the fuel-cell pwer rating reduced from 300 kW to 250 kW**.**

Figures 13 and 14 show the effects of reducing the fuel cell power level to 250 kW and, as would be expected, these plots indicate that the stored energy in the battery is depleted to a much greater extent (23 kWh), with the maximum rate of discharge increasing to about 4kWh/minute. This suggest that long clmbs on steep gradients must lead to a significant depletion of stored battery energy and this has a direct effect on the battery storage capacity that must be provided.

5.1.2 Inverse simulation results

As mentioned in Section 4.2, the specific approach to inverse simulation used in this work involves high-gain feedback system principles. For this application, as shown in Figure 15, the feedback loop involves taking the difference between the desired distance data record, $x_{ref}(t)$ (obtained from the Class 156 dmu simulation discussed in the Appendix) and the corresponding distance, $x_{inv}(t)$, from the model of the hybrid multiple unit. The feedback equation takes the form:

$$T_{inv}(t) = K\left(x_{ref}(t) - x_{inv}(t)\right) \tag{6}$$

where the gain factor K is chosen on a trial and eror basis, guided by experience gained from other practical applications of ivnerse simulation. In this case a value of of 10^8 has been found to be satisfactory. The variable $T_{inv}(t)$ is the tractive force needed to satisfy the given distance versus time data set used as reference input $x_{ref}(t)$. Details of the parameter values used for the simulation of the dmu and a typical set of results may be found in the Appendix. In addition to the tractive force, other output variables that could be obtained from the inverse simulation are the distance travelled, speed, instantaneous power level at the rail or at the battery terminals, or the energy expended in matching the given desired distance time history used as reference input.

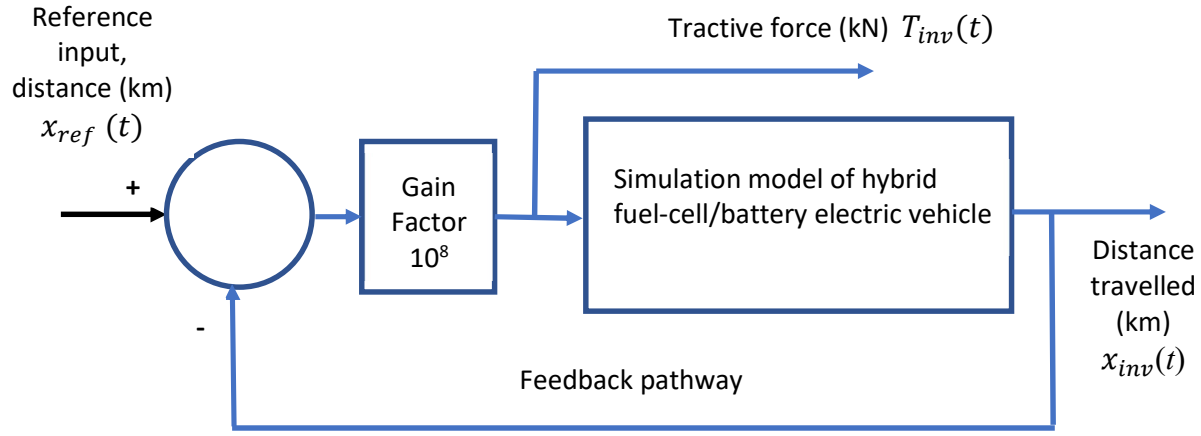

Figure 15: Block diagram illustrating the application of the high-gain feedback approach to inverse simulation as applied to the model of the hybrid fuel-cell/battery electric multiple unit. The inverse simulation is formed by the complete feedback system. The reference input is the desired distance/time record, while the output variable of the inverse model is the tractive force developed by the hybrid vehicle.

Figure 16 shows a typical distance versus time data record used as the reference input $x_{ref}(t)$. Changes in the gradient of this record correspond to changes in speed. It can be seen from Figure 16 that the train comes to a halt approximately 15 km from the starting point. The high-gain of the feedback loop forces the model of the hybrid fuel-cell/battery electric unit to follow the reference input almost exactly, with the difference between the two distance records being less than 0.0006 m at all times, as shown in Figure 17. The high frequency oscillations that appear on this difference record are a feature of this inverse simulation method and of the methods of numerical integration being employed. Such transient oscillatory behaviour is not significant and does not cause problems in terms of the interpretation of results from the inverse simulation.

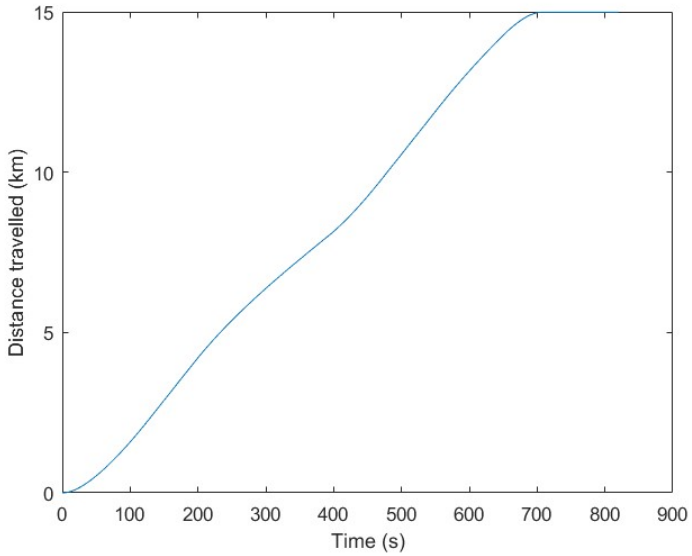

Figure 16: Reference input used for inverse simulations, as obtained from a simulation run of the Class 156 dmu for the test route. This record is the same as that shown in Figure A4 of the Appendix.

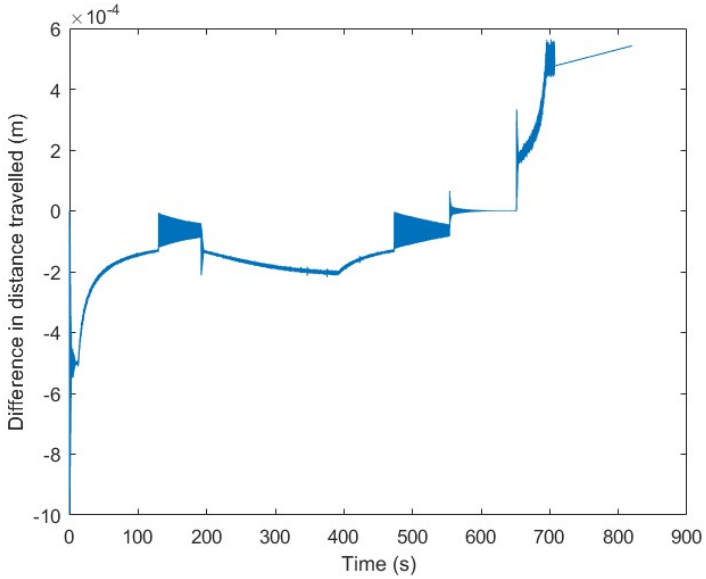

Figure 17: Plot of difference values (m) in terms of reference distance and distance travelled by hybrid multiple unit, as obtained from inverse simulation. Parameter values for the model of the hybrid unit are as shown in Table 1.

Figure 18 is the speed versus time record corresponding to Figure 16 and this is similar in shape to the forward simulation result for the hybrid unit, as shown in Figure 5. However, it should be noted that the journey times are not exactly the same in the two cases, with the inverse simulation showing that the train comes to rest in 708 s, as opposed to 678.5s in the forward simulation. This is because, unlike the case of the forward simulation model where inputs were the tractive force or power level, the inverse simulation is being driven from the distance versus time curve for the Class 156 dmu. The journey time for the hybrid multiple unit is therefore the same as for the dmu and the speed and distance versus time plots are the same as those in Figures A3 and A4 respectiely.

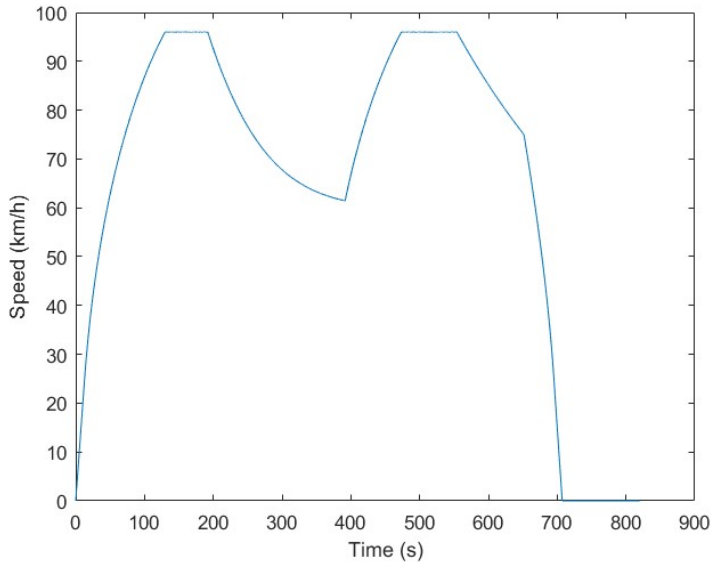

Figure 18: Record of speed (km/h) versus time (s) obtained from inverse simulation of the hybrid multiple unit for parameter values given in Table 1.

Figure 19 shows the inverse simulation result for the tractive force in the hybrid multiple unit and this can be seen to be similar in shape to the equivalent forward simulation record in Figure 7. The same is true of other variables, such as power at the rail and the battery power, although these records all involve numerical values that differ slightly from those found from the forward simulation due to the fact that the journey times are not the exactly same in the two cases.

Figure 20 shows the record of stored energy in the battery and this is again similar in shape to the record in Figure 10. However, the battery discharge rate when the train is accelerating or ascending the gradient is less than in the forward simulation. This is consistent with the fact that the power at the rail is about 50 kW less for the conditions applying in the inverse simulation. This reduces the requirement from the battery by the same amount and hence reduces the rate of change of the stored energy when the battery is discharging.

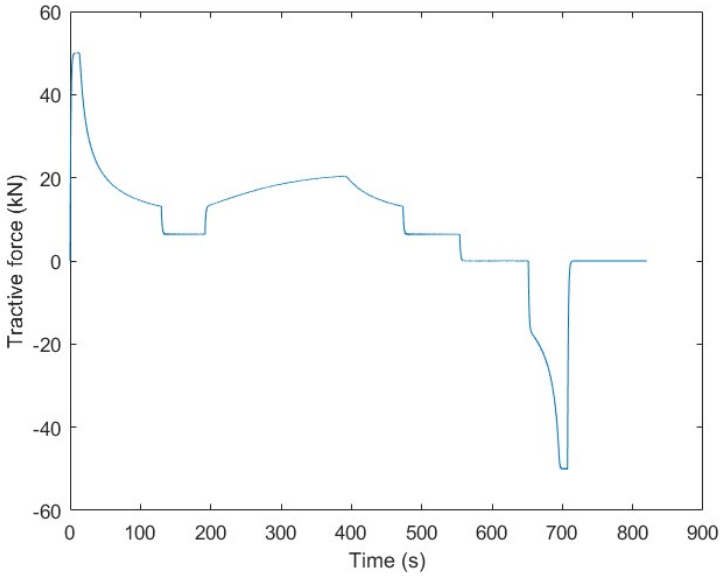

Figure 19: Record of tractive force (kN) versus time (s) obtained from the inverse simulation of hybrid multiple unit for parameter values given in Table 1.

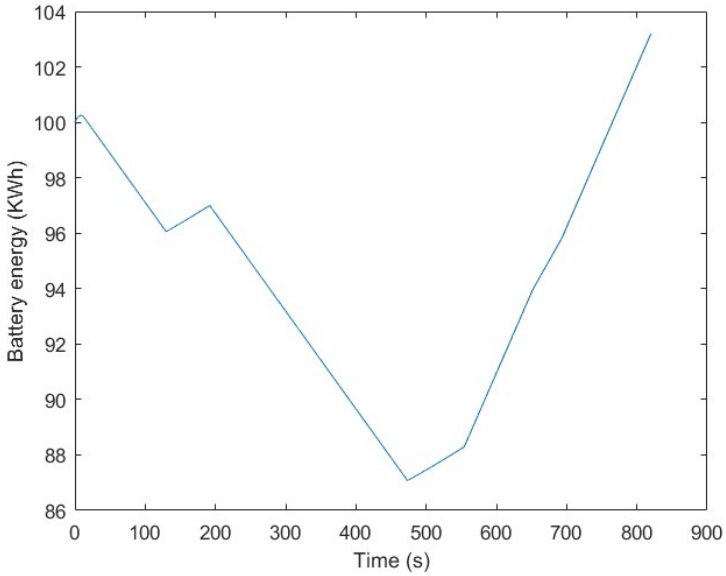

Figure 20: Record of battery energy for hybrid vehicle as obtained from inverse simulation for parameter values as given in Table 1.

What is of special interest in the inverse simulation is investigation of the way in which the battery performance changes when model parameters are changed, for a fixed distance and journey time. For example, Figures 21 and 22 show the effect on the stored energy in the battery of a small change in the mass of the train. In Figure 21 an increase of mass of 10 tonnes leads to an increase in the energy drawn from the battery to maintain the reference schedule. The minimum value of stored energy in Figure 21 is therefore smaller than that shown in Figure 20. For a reduction of mass of 10 tonnes the minimum value of stored energy, as shown in Figure 22, is slightly greater than in the case considered in Figure 20 for the 90-tonne value.

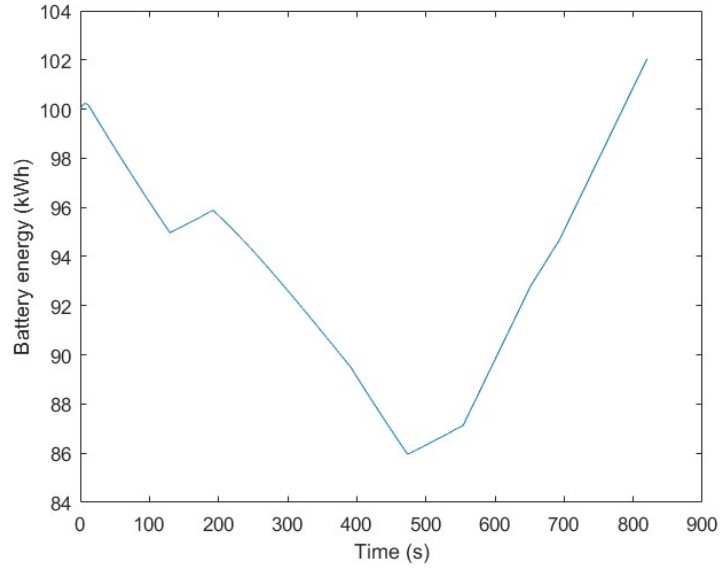

Figure 21: Record of battery energy for hybrid vehicle as obtained from inverse simulation for parameter values as given in Table 1 but with train gross weight increased to 100 tonnes.

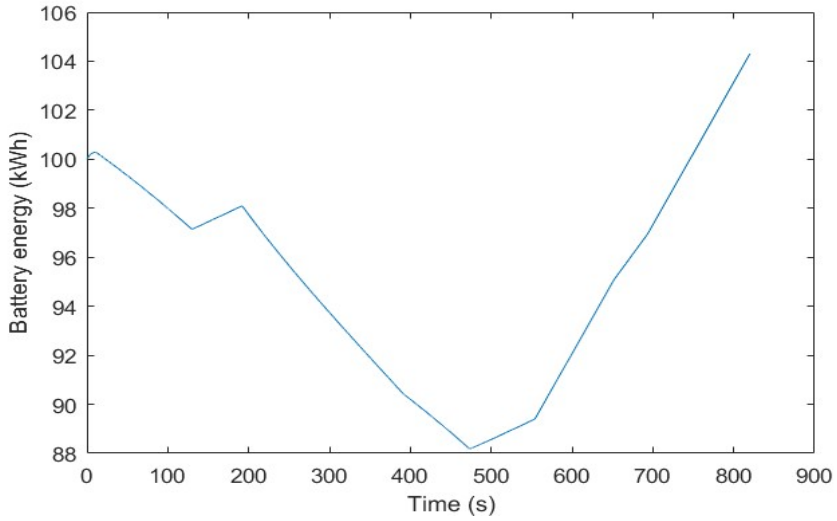

Figure 22: Record of battery energy for hybrid vehicle as obtained from inverse simulation for parameter values as given in Table 1 but with train gross weight reduced to 80 tonnes.

Inverse simulation methods also allow examination of the effects of increasing or reducing the time required for the journey. The distance versus time record obtained from the reference simulation of the diesel multiple unit can be adjusted very easily using concepts of time scaling that have been used routinely within the computer simulation field since the days when electronic analogue computers were widely used [43]. Time scaling simply involves the introduction an additional gain factor for each separate integration operation and can be done easily for a simulation model in MATLAB®. For example, a factor of 1.05 associated with each integrator in a simulation model reduces the simulated time for that model by 5% and, similarly, a factor of 0.95 increases the time by the same percentage. Time scaling is usually applied uniformly over the whole period of the simulation but may, in principle, be applied for a part of the record only, such as during braking.

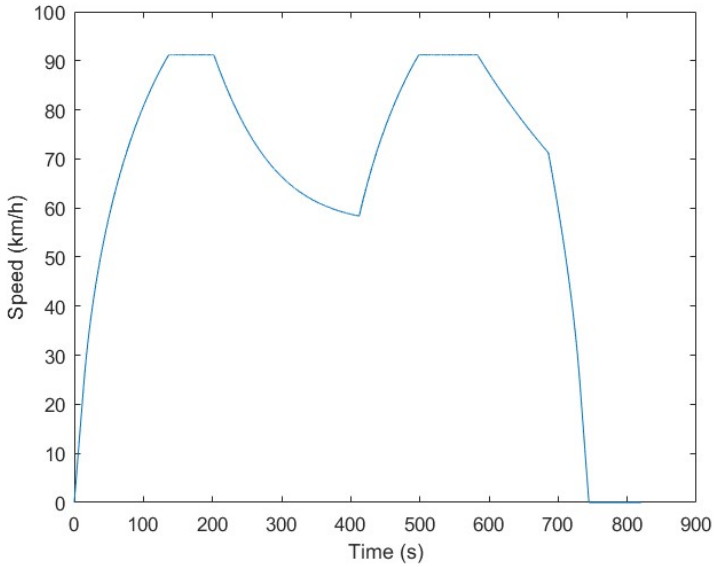

Figure 23: Record of speed versus time for hybrid vehicle obtained from inverse simulation for the chosen route (for parameter values as given in Table 1) with a distance versus time record from the Class 156 dmu simulation as the reference input. In this case time scaling has been applied to the reference input time history to give an increase of 5% in the journey time.

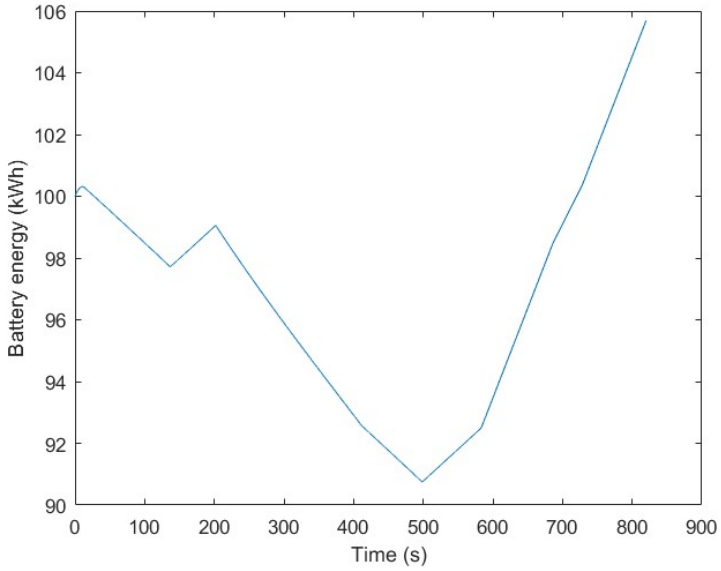

Figure 24: Record of battery stored energy versus time for the hybrid vehicle obtained from inverse simulation for the chosen route (for parameter values as given in Table 1) with a distance versus time record from the Class 156 dmu simulation as the reference input. As in Figure 23, time scaling has been applied to the reference input time history to give an increase of 5% in the journey time.

Figure 23 shows a speed versus time record for a 5% increase in travel time (about half a minute) for the given route. Figure 24 shows the corresponding record for stored energy in the battery and, compared with Figure 11, this shows a reduction in energy drawn from the battery during the period when the train is climbing the 1 in 50 gradient from about 10 kWh to approximately 6 kWh. On the other hand, a 5% reduction in travel time would lead to speeds that exceed the maximum line speed and an increase in energy drawn from the battery. This process of time scaling is potentially useful in considering the energy costs associated with possible journey time reductions. Equally, it can be used to provide useful information about the potential benefits of revised coasting or braking strategies.

One practical issue that has not been considered in the simulation work concerns the fact that any changes in battery storage capacity, fuel-cell power output or traction motor ratings have immediate consequences in terms of the mass of the train and also space requirements for equipment in the roof areas or below the floor. Linking of train weight, component ratings and space requirements within the simulation model is therefore an area for further work. This should not be too difficult, provided components are chosen from commercial products that are currently available, for which weight and volume information can be found (see e.g. [16]).

Although the use of the inverse simulation approach introduces additional complexities in terms of system modelling and simulation, the fact that it allows comparisons to be made of performance for different parameter values for a fixed journey distance and time is important. Time scaling allows investigation of the effect of reducing or increasing the journey time and this is also important. Using inverse simulation, one can see immediately the full effects of parameter and schedule changes and whether these can be accommodated within the limits of the available power at the rail, the line speed restrictions and the braking rates allowed. Conventional forward simulation methods could certainly be used for investigations such as these, but they involve more tedious and time-consuming trial and error procedures to gain the same level of insight. Experience suggests that, in practice, a combination of inverse and conventional simulation methods can often prove beneficial.

6. Discussion of results in the context of routes in Scotland.

It is possible to extrapolate from the simulation results presented in Section 5 to allow an assessment to be made of the characteristics of hybrid multiple units needed for routes such as the West Highland line. Typical sections of the West Highland line involve prolonged climbs where battery power could be used to augment the energy from the fuel cell and also long descents where the battery would be charged from the fuel cell. One demanding part of the line which is encountered by trains bound for Fort William is the section between Ardlui and the summit beyond Upper Tyndrum. Another has to be tackled by Glasgow-bound trains between Spean Bridge and the summit near Corrour station. In the former case the distance involved is 24.8 km and the gradient profile shows that, apart from a short downhill section of about 1.3 km at Crianlarich station, the gradient is close to 1 in 60 uphill for almost all of that distance. The current working timetable shows that trains are allowed 15½ minutes for the section from Ardlui to Crianlarich (approximately 14 km) and 8½ minutes from Crianlarich to Upper Tyndrum (about 5 km). For the 29.6 km section from Spean Bridge to Corrour the rising gradient is continuous, almost all the way to Corrour station. Over the two short sections to Roy Bridge and then on to Tulloch the gradients vary from 1 in 188 to 1 in 64 but, beyond Tulloch, the route then steepens to involve long sections at 1 in 59, 1 in 67 and finally at 1 in 57 before the summit. The timings from Spean Bridge are 6 minutes to Roy Bridge, a further 10 minutes to Tulloch and then 16 minutes to Corrour station (about ½ km past the summit of the line).

The test route described in Section 3 involves a gradient of 1 in 50, which is steeper than the specific sections of the West Highland line mentioned above but is still typical of other sections of that route and of other routes in Scotland. Sections 5.1 and 5.2 include graphs showing the variations in stored battery energy for a number of different hybrid train configurations. The results suggest that with two 200 kW traction motors, a hydrogen fuel cell of 300 kW output and a battery providing a maximum power output of 250 kW, the stored energy in the battery falls at a rate of about 3 kWh/minute during the climb (Figure 10). Increasing the fuel cell power rating to 350 kW gives a battery stored charge reduction rate of just over 2kWh/minute (Figure 11) while reducing it to 250 kW increases this value to about 4 kWh/minute (Figure 13).

Repetition of the simulation with the parameter values as given in Table 1, but with a slightly altered test route where there is a gradient of 1 in 60 instead of 1 in 50 brings the loss of stored energy during the climb down to only 2.1 kWh/minute instead of the previous 3 kWh/minute. Thus, over the 15½ minutes between Ardlui and Crianlarich, the battery energy would decrease by about 32.5 kWh. Continuing to Upper Tyndrum, the energy cost is close to 18 kWh giving a total of about 50.5 kWh between Ardlui and Upper Tyndrum. Stored energy would be recovered at a rate of 3.5 kWh/minute during braking and when the train is at rest at Crianlarich station. Howeer, it should be noted that, at most stations the scheduled dwell times are of the order of 1½ or 2 minutes at most and, accordingly, a dwell time of only two minutes has been allowed at Crianlarich, assuming that the train is not being divided there into Oban and Fort William sections. Thus between departure from Ardlui and departure from Upper Tyndrum, for a total travelling time of 24 minutes for the 22 km, there would be about 3 to 4 minutes of charging during dwell times and also about 4 minutes charging during coasting or braking. This section of the route could therefore involve 20 minutes of battery discharge at about 2.1 kWh/minute and up to 8 minutes of charging at 3.5 kWh/minute to give a net cost in terms of stored energy of just over 12 kWh. The true cost would, in fact be greater because of the periods of acceleration after the stations at Ardlui and Crianlarich and, using information from the simulation runs, an overall figure of just over 20kWh might be a more realistic estimate for the total energy cost. Similarly, in the southbund direction, an estimate of the stored energy cost for the 29.6 km and 32 minutes of travelling time between Spean Bridge and Corrour is about 35 kWh. This figure allows for 2½ minutes of dwell time and 5 minutes of coasting or braking and takes account of the additional energy costs of acceleration following departure from the stations. This estimated figure also makes allwance for the fact that, on this section of the route, the average gradient is not as steep as 1 in 60.

Downhill sections of the route, together with stations stops and braking, provide many opportunities for battery charging but it is clear that stored battery energy of at least 35 kWh must be available to deal with the long climb from Spean Bridge to Corrour. If the train did not stop at Roy Bridge and Tulloch the stored energy would be depleted by an additional 9 kWh, at least. It should be noted that the simulation does not (in its present form) take account of the effect of local speed restrictions and the train performance model does not allow for increased resistance on curved track which would introduce further demands in terms of power. If these features were included in the simulation the demands in terms of stored energy from the battery would increase on uphill sections of the route. It is therefore suggested that, allowing for an appropriate safety margin, the battery should be chosen to give a storage capacity of at least 75 kWh for the chosen fuel cell power rating of 300 kW and battery power rating of 250 kW.

As was shown in the forward simulation reults in Figure 11, an increase in fuel cell power rating from 300 kW to 350 kW leads to a reduction in the rate of energy loss from the battery on the 1 in 50 gradient section by about one third and this suggests that use of a fuel cell power rating which is greater than the nominal 300 kW of Table 1 might be useful. Using the test route profile with a 1 in 60 gradient, which is more typical of the sections of the West Highland line discussed here, the inverse simulation model can be used to investigate the possible benefits and costs in terms of stored energy of increasing the fuel cell power rating and, at the same time, reducing the journey time. Figure 25 shows the pattern of stored energy in the battery versus time for the nominal journey time and the parameter values of Table 1 and indicates that the rate of loss of battery energy is 2.11 kW/minute. The equivalent figure found for a fuel cell power rating increased from 300 kW to 350 kW is 1.28 kWh/minute. Figure 26 shows equivalent results for a case involving the 350 kW fuel cell and a reduction of journey time of 10%. This cuts about one minute from the schedule and gives a rate of stored energy loss during the 1 in 60 climb of 2.25 kWh/minute, which represents only a small increase from the 2.11 kWh/minute value found for the case involving the 300 kWh fuel cell for the nominal schedule.

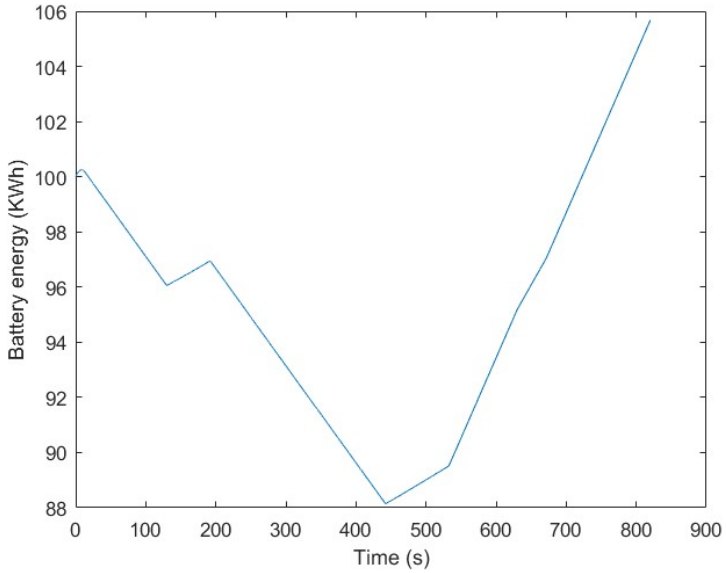

Figure 25: Record of battery stored energy versus time for the hybrid vehicle obtained from inverse simulation for the chosen route with a 1 in 60 gradient (for parameter values as given in Table 1). The distance versus time record from the Class 156 dmu simulation provides the reference input, generated using the same 1 in 60 gradient profile.

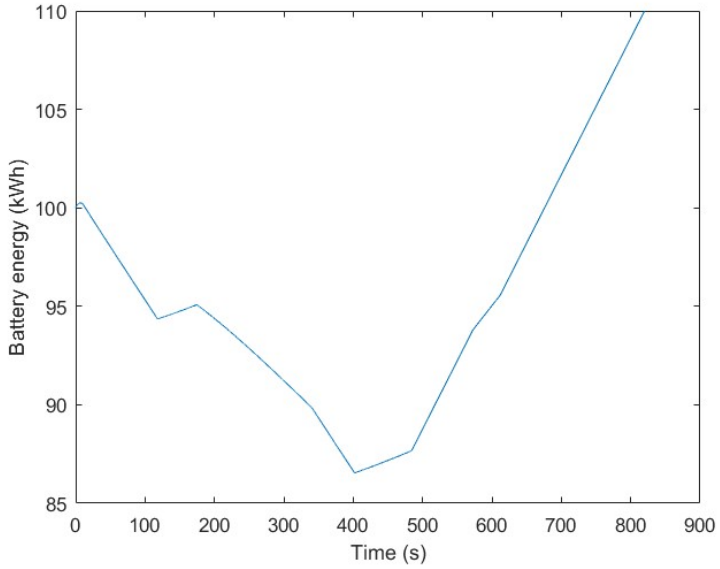

Figure 26: Record of battery stored energy versus time for the hybrid vehicle found using inverse simulation for the test route with a 1 in 60 gradient section (for a fuel cell rating of 350 kW and other parameter values as given in Table 1). As in the case of Figure 25, the reference distance versus time record from the Class 156 dmu simulation has been used as input. In this case time scaling has been applied in the dmu simulation to give a reduction of 10% in the journey time.

The analysis presented above, although based on approximate calculations which depend on simulation evidence involving the simplified test route, suggests that a combination of a 350 kW fuel cell and a 250 kW battery with a storge capacity of 75 kWh might provide a more suitable configuration of the powertrain elements in a hybrid multiple unit than the equivalent parameter values in Table 1. More detailed assessment would be needed using a simulation model involving a detailed profile of the West Highland line, incorporating all gradient changes and local speed restrictions. This would also allow the costs and benefits of a possible reduction in journey time over specific sections of the route to be investigated using time scaling.

The train weight for the chosen powertrain configuration requires careful consideration. The nominal value of the train weight shown in Table 1 is 90 tonnes. This figure has also been used for the weight of the Class 156 unit in the Appendix and is an estimate of gross weight, allowing for a full train load of passengers with luggage. Subtracting the weight of the diesel engines, fuel tanks, driveshaft, transmission system and all the associated equipment would reduce the weight of a Class 156 unit by just over 10 tonnes [16]. Thus the weight of the traction motors, fuel cell, battery and other equipment for the proposed two-coach hybrid multiple unit should, ideally, be of the order of 10 tonnes or less. Using standard commercial items [16] capable of meeting the requirements estimated above, the weight of the main powertrain elements are as follows:

- Four 104 kW fuel cell units and associated equipment (such as air blower, coolant pump and dc/dc converter) – 2000kg.
- Four 22 kWh battery pack units and associated thermal management system - 2600 kg.
- Two traction motors at 600 kg each – 1200kg.
- IGBT power electronic converters - 1700 kg.
- Other equipment such as hydrogen storage tanks, compressor and associated pipework 1800kg

This would give an estimated total weight for the powertrain equipment of about 9.3 tonnes which is close to the weight of all the equipment associated with the engines, driveshaft and transmission components of the Class 156, as detailed above . However, it should be emphasised that no attempt has been made to estaablish whether or not all this powertrain equipment could be accommmodated within

a two-coach hybrid unit. The provision of a pantograph and asociated circuit breaker and transformers would give a hybrid unit much added flexibility in terms of its operation but would add about 4 tonnes to the weight and would also add to the problems of finding space for the equipment.

7. Proposals for further work

The first prioirty is to extend the modelling work using a more detailed route profile based on a section of a real route in Scotland. The West Highland line is probably the most suitable example to consider as it is a long route with significant gradients. The route models would have to include all gradient changes, local speed restrictions and relevant information about curvature of the line to allow the resistance forces to be calculated more accurately. Such a simulation model could then be used to extend the work discussed in Section 6 and allow the preliminary conclusions presented there to be reassessed.

Since three-coach hybrid units with 90 mph (144 km/h) capabilities might be required for use on some routes in Scotland, it would also be useful to carry out simulation studies involving a model of a three-coach hybrid unit. This could be equipped with pantograph and transformer to allow it to draw power from 25kV overhead lines when used on electrified routes. As indicated in Section 6, this additional equipment would add about 4 tonnes to the weight of the train but could be a useful feature that would extend considerably the capabilities of the hybrid multiple units.

Another useful extension of the existing simulation model could involve linking battery storage-capacity, fuel-cell power output, traction motor ratings and hydrogen storage tank characteristics to the overall train weight. Any changes made to the simulation model, in terms of power ratings or energy storage capacities, could then lead automatically to changes in the total weight of the train and any violation of constraints in terms of the volume of components in relation to the space available could be flagged-up for the user's attention. This should not present major difficulties, provided weight and volume information is available for the components.

As mentioned in Section 2, development of a more complex, physics-based, representation would be useful. This was not considered necessary for the limited objectives of the current investigation, but it would certainly be useful to have physics-based mathematical models available for the main powertrain sub-systems for future simulation work. This could allow some of the fundamental assumptions made in the development of the existing simplified model to be more fully assessed. For example, the assumption that the fuel cell should be operated in a steady state condition for almost all of the time in order to avoid changes in fuel cell loading and the associated sluggish dynamic response could be investigated in detail. This could be helpful in reaching conclusions about the correctness or otherwise of the assumption that a steady state operating condition for the fuel cell is optimal.

A complete train model built up of a set of detailed dynamic sub-models of that kind might lead to a simulation involving much longer computation times than the present model, since it would have to represent both the very fast switching action of power-electronic components and also the much slower dynamics associated with the processes within the batteries and fuel-cell. However, techniques of multi-rate simulation that have proved useful in other fields [44] could be used to overcome this difficulty. The extended simulation model could also be of value for the development of control and energy management strategies. It is proposed therefore that generic physics-based models be developed for the three main sub-systems (fuel cell, battery and traction motors) , together with more detailed models of the power-electronic inverters and dc/dc converters.

This report considers only hybrid powertrain configurations involving hydrogen fuel cells and batteries. However, it is important that the potential of supercapacitors for energy storage should not be neglected for the type of application being considered here. The long ascents and descents on Scottish rural railways involve a situation which differs greatly from the urban routes where supercapacitors have attracted most attention Nevertheless, it would be interesting to examine a coordinated hybrid

configuration involving both supercapacitors and batteries. Quantitative insight about the possible value of this type of configuration could be gained by integrating a supercapacitor sub-system into the existing simulation model structure. This might require the use of more detailed component sub-models and should be linked to the development of dynamic physics-based sub-system descriptions.

8. Conclusions

In considering possible specifications for hybrid fuel-cell/battery electric multiple units there is a clear need for high levels of transient power and large amounts of stored energy on routes that involve steep and prolonged gradients. Simulation techniques allow fundamental design options for hybrid rail vehicles to be assessed quickly and easily using relatively simple mathematical models. It is suggested that the use of inverse simulation techniques provides insight that is not so readily available using conventional simulation methods alone. The use of an approach based on a combination of forward and inverse methods is therefore recommended for future investigations.

The analysis within Section 6 of this report shows that approximate calculations of energy usage, found by extrapolation from simulation results obtained from a simplified model and test route, can provide useful insight. From this analysis it is suggested that a specification for a hybrid two-coach unit could involve two 200 kW traction motors, fuel-cells providing a maximum power output of 350 kW and a battery pack providing a 250 kW maximum output and 75 kWh of storage capacity. Using standard components that are available commencially, approximate calculations suggest that a design based around these figures could be implemented within a target weight of 90 tonnes for a two-coach unit. However, the limitations of the UK loading gauge are likely to present difficulties in terms of the amount of space required and implementation might only be possible at the cost of passenger space. Further calculations based on precise component dimensions are needed to investigate that issue in detail, but it is also important to recognise the fact that the power densities of fuel cells and batteries are improving steadily. Much research and development work is also under way aimed at improving the specific (gravimetric) and volumetric energy densities of batteries and also at improving on-board hydrogen storage systems. Such developments could mean that a specification of the kind oulined above could be implemented more easily in the not too distant future. It is also suggested that a possible three-coach solution be considered in further simulation studies and that the addition of a pantograph and associated equipemt to allow the unit to draw power from overhead wires on 25 kV electrified routes would be a useful additional feature to be cnsideed in future simulation work.

As well as conventional hydrogen fuel cells, batteries and supercapacitors, there are other developments that must not be neglected. For example, much useful experience has been gained elsewhere with methods of short-term energy storage based on flywheels and hydraulic systems [29]. Simulation techniques could allow these to be compared in a quantitative way with battery or supercapacitor-based energy storage systems. New developments in hydrogen-based technology also need to be considered, such as the development work, led by engineers at Steamology Motion Ltd on a so-called “Water 2 Water” system. This involves a turbine that runs on high pressure steam generated by combining hydrogen and oxygen The development work has recently been given a UK Government grant of £350,000 by the Department for Transport and the approach is currently being assessed for possible use as a range extender for the Vivarail Class 230 battery-electric unit [45].

Finally, it must be recognised that technology is changing fast and also that much of the present-day research and development effort on hydrogen fuel cells and batteries is driven by automotive industry requirements. However, trains provide a much more demanding application, one key difference being that a typical daily operating period for a train is about 16 hours compared with the daily average use of or two hours for private cars. It is important, therefore, that more future research and development effort on novel forms of powertrain be devoted specifically to railway applications. Given the high cost of developing prototype systems for evaluation on the rails, it is also important that the potential of simulation methods in this field should be more widely recognised.

The issues highlighted in this report suggest that design specifications for hybrid multiple units for use on non-electrified routes in Scotland are especially demanding, due to the distances involved and gradients encountered. However, it must be recognised that any trains designed specifically for such routes are unlikely to be commercially viable due to the relatively small number of units needed and the inevitable infrastructure costs of providing hydrogen storage and re-fuelling points. Similar issues of long journeys and steep gradients will be encountered in considering the needs of some routes in Wales and in parts of England, such as between Settle and Carlisle. It is therefore important that those involved in development and design activities in connection with fuel-cell/battery-electric rail vehicles for use in the United Kingdom take full account of the characteristics of routes in the highlands of Scotland when defining performance specifications.

9. Acknowledgements

I wish to thank members of the Scottish Association for Public Transport who have expressed interest in this work and also for the helpful feedback that some have provided following the publication of the two earlier reports ([28] , [29]). I would also like to thank Mr Scott Prentice, Head of Business Development, ScotRail, for his interest and for providing useful technical information concerning the performance characteristics of Class 156 diesel multiple units.

References

1. Anonymous (2020). *Decarbonising Transport: Setting the Challenge*. Policy paper. UK Department of Transport, 26th March 2020. Online: www.assets.publishing.service.gov.uk . Accessed 06/05/2020.
2. Anonymous (2019). *Rail Industry Decarbonisation Taskforce – Final Report for the Minister for Rail*. Online: www.rssb.co.uk . Accessed 06/05/2020.
3. Anonymous (2019). *Options for Traction Energy Decarbonisation in Rail: Final Report (T1145 Report)*. RSSB 2019. Online: www.catalogues.rssb.co.uk . Accessed 06/05/2020.
4. Anonymous (2019). *Carbon Account for Transport No. 11, 2019 Edition*. Transport Scotland. 2019. Online: www.transport.gov.scot . Accessed 07/05/2020.
5. Anonymous (2019). *Scotland's Future: The Government's Programme for Scotland 2019-2020.* 3rd September 2019, Scottish Government website. Online: https://www.gov.scot/publications/protecting-scotlands-future-governments-programme-scotland-2019-20/ . Accessed 07/05/2020.
6. Clinnick R (2020). Trial to convert Class 314 EMU to hydrogen power. *Rail*, Issue 900, (March 11-March 24, 2020), 28-29.
7. Anonymous. *Battery Multiple Unit – Derby 2-car BMU*. Railcar.co.uk website. Online: www.railcar.co.uk/type/battery-multiple-unit . Accessed 10/05/2020.
8. Murray-Smith D (2018). *Aberdeen to Ballater by BMU: notes on the battery railcar experiment.* Article, Railscot website. Online: www.railscot.co.uk/articles/Aberdeen_to_Ballater_by_BMU:_Notes_on_the_Battery_Railcar_Experiment/ . Accessed 10/05/2020.
9. Anonymous (2015). *Batteries included: Prototype battery-powered train carries passengers for first time*. Network Rail Media Centre News Report, 13th January 2015. Online: https://www.networkrailmediacentre.co.uk/news/batteries-included-prototype- battery-powered-train-carries-passengers-for-first-time Accessed 10/05/2020.
10. Murray-Smith D J (2018). Battery electric train demonstration: Vivarail 2030 BEMU on the Bo'ness and Kinneil Railway. *Scottish Transport Matters, Newsletter, Scottish Association for Public Transport*, 180; 2018-4: 5. Online: http://www.sapt.org.uk/Newsletter2018-4.pdf Accessed 10/05/2020.
11. Anonymous (2020). Ready to charge. *Rail*, Issue 900, (March11-March24, 2020), Special Report (Decarbonisation Special), 42-43.

12. Anonymous (2018). BatteryFLEX Desiro EMU conversion proposed. *Railway Gazette.* 15th October 2018. Online: www.railwaygazette.com/uk/batteryflex-desiro-emu-conversion-proposed/47363.article Accessed 10/05/2020.
13. Shirres D (2019). Hitachi plans to run ScotRail Class 385 EMUs beyond the wires. *Rail Engineer.* Online: www.railengineer.co.uk/2019/03/26/hitachi-plan-to-run-scotrail-class-385-emus-beyond-the-wires/ . Accessed 10/05/2020.
14. Anonymous (2018). ŐBB and Bombardier sign call-off order for 25 TALENT 3 trains. *Global Railway Review,* 3rd July 2018. Online: www.globalrailwayreview.com/news/70893/obb-bombardier-25-talent-3-trains/ Accessed 10/05/2020.
15. Burrows A and Hillmansen S (2020) Full steam ahead, *Rail*, Issue 900, (March11-March 24, 2020), Special Report (Decarbonisation Special), 40-41.
16. Kent S, Gunawardana D, Chicken T and Ellis R (2016). *Future Railway Powertrain Challenge: Fuel Cell Electric Multiple Unit (FCEMU) Project. FCEMU Project-Phase 1 Report-Issue 1.* University of Birmingham, Hitachi Rail, Fuel Cell Systems Ltd., June 2016. Online: www.birmingham.ac.uk/Documents/college-eps/railway/1-Class-156-Fuel-Cell-Electric-Multiple-Unit-Feasibility-Study-Issue-1.pdf Accessed 10/05/2020.
17. Anonymous (2018). *Coradia iLint – the world's first hydrogen powered train.* Alstom website. Online: https://www.alstom.com/our-solutions/rolling-stock/coradia-ilint-worlds-1st-hydrogen-powered-train Accessed 10/05/2020.
18. Barrow K (2019). Vivarail forms hydrogen fuel-cell partnership, *International Rail Journal*, May 8th 2019. Online: www.railjournal.com/fleet/vivarail-forms-hydrogen-fuel-cell-partnership/ . Accessed 10/05/2020.
19. Anonymous (2019). *HydroFLEX Hydrogen Train.* Railway Technology website. Online: https://www.railway-technology.com/projects/hydroflex-hydrogen-train/ Accessed 10/05/2020.
20. Anonymous (2019). New hydrogen "Breeze" trains unveiled by Alstom and Eversholt. *Rail Technology Magazine*, 17th January 2019. Online: www.railtechnologymagazine.com/Rail-News/new-hydrogen-breeze-trains-unveiled-by-alstom-and-eversholt . Accessed 10/05/2020.
21. Reidinger E (2019). Zillertalbahn hydrogen train design revealed, *International Railway Journal*, February 18th 2019. Online: www.railjournal.com/fleet/zillertalbahn-hydrogen-train-design-revealed/ Accessed 10/05/2020.
22. Zenith F, Møller-Holst S and Thomassen M (2017). *Alternative railway electrification in Norway,* Paper presented at FCH 2JU & S2R JU "Hydrogen Train Workshop", Brussels, May 15th 2017. Online; www.sintef.no/en/projects/hydrail/ Accessed 10/05/2020.
23. Zenith F, Isaac R. Hoffrichter A, Thomassen M S and Møller-Holst S (2020). Techno-economic analysis of freight railway electrification by overhead line, hydrogen and batteries: Case studies in Norway and USA. *Proc IMechE Part F: J Rail and Rapid Transit,* 2020;; 234, 7:791-802. doi: 10.1177/0954409719867495. Available online: https://journals.sagepub.com/doi/pdf/10.1177/0954409719867495 Accessed 20/06/2020.
24. Shirres D and Baxter J (2019). *The future of hydrogen trains in the UK,* Report, Institution of Mechanical Engineers, London, 2019. Available online: https://www.imeche.org/policy-and-press/reports/detail/the-future-for-hydrogen-trains-in-the-uk Accessed 20/06/2020.
25. Zhao H and Burke A F (2010). Fuel cell powered vehicle using supercapacitors- device characteristics, control strategies and simulation results. *Fuel Cells,* 2010; 10, 5: 879-896.
26. Barrow K (2014) CSR unveils 100% supercapacitor powered tram. *International Railway Journal.* May 29th2014. Online: https://www.railjournal.com/passenger/light-rail/csr-unveils-100-supercapacitor-powered-tram/ Accessed 20/06/20.
27. Zhang H, Yang J, Zhang F, Song P and Li M (2020). Optimal energy management of a fuel-cell-battery-supercapacitor powered hybrid tramway using a multi-objective approach. *Proc IMechE. Part F: J Rail and Rapid Transit* 2020; 234, 5: 511-529. First published online 15th May 2019.

28. Murray-Smith D (2019). *Powering Future Transport in Scotland*, A report for the Scottish Association for Public Transport, June 2019. Available online: http://eprints.gla.ac.uk/189828/1/189828.pdf . Accessed 24/06/20.
29. Murray-Smith D (2019). *A Review of Developments in Electrical Battery, Fuel cell and Energy Recovery Systems for Railway Applications,* A report for the Scottish Assciation for Public Transport, November 2019. Available online: http://eprints.gla.ac.uk/204435/1/204435.pdf. Accessed 24/06/20.
30. Murray-Smith D J (2018) Development of an inverse simulation method for the analysis of train performance, *Proc IMechE Part F: J Rail and Rapid Transit,* 2018, Vol. 232(5) 1295–1308. DOI: 10.1177/0954409717720349. First published in electronic form, 14th July, 2017. Available online: http://eprints.gla.ac.uk/148116/1/148116.pdf . Accessed 24/06/20.
31. Douglas H, Weston P, Kirkwood D, Hillmansen S and Roberts C, (2017), Method for validating the train motion equations used for passenger rail vehicle simulation, *Proc IMechE Part F: J Rail and Rapid Transit*, 2017; 231(4): 455-469. Available online: https://journals.sagepub.com/doi/abs/10.1177/0954409716631784 Accessed 20/06/2020
32. Salvador P, Martinez F, Villalbo I and Insa R (2018). Modelling energy consumption in diesel multiple units. *Proc IMechE Part F: J Rail and Rapid Transit,* 2018; 232(5): 1539–1548. First published online 31st October 2017.
33. Murray-Smith D J (2015). *Testing and Validation of Computer Simulation Models, Principles, Methods and Applications.* Springer: Cham, Switzerland, 2015. ISBN 9783319150994 (doi:10.1007/978-3-319-15099-4)
34. Beisbart C and Saam N J (eds.) (2019). *Computer Simulation Validation: Fundamental Concepts, Methodological Frameworks, and Philosophical Perspectives.* Springer: Cham, Switzerland, 2019. ISBN 9783319707655 (doi:10.1007/978-3-319-70766-2_4).
35. Mathworks Inc. *MATLAB®/Simulink® modelling and simulation software.* http://www.mathworks.com/products/. Accessed 10 May 2020.
36. Campbell S L, Chancelier J-P and Nikoukhah, R. (2000). *Modeling and Simulation in Scilab/Scicos*, Springer: New York, NY, USA, 2000.
37. Thomson D and Bradley R (2006). Inverse simulation as a tool for flight dynamics research - Principles and applications. *Prog. in Aerospace Sciences*, 2006; 42: 174-210.
38. Hess R A, Gao C and Wang S H (1991). A generalized technique for inverse simulation applied to aircraft maneuvers. *AIAA J Guidance Control and Dynamics,* 1991; 14: 920–926.
39. Thomson D G and Bradley R (1998). The principles and practical application of helicopter inverse simulation. *Simulation Practice and Theory,* 1998; 6: 47–70.
40. Murray-Smith D J (2000). The inverse simulation approach: a focused review of methods and applications, *Mathematics and Computers in Simulation,* 53:239-247, 2000. Available online: https://www.sciencedirect.com/science/article/abs/pii/S037847540000210X?via%3Dihub Accessed 24/06/20.
41. Buchholz J J and von Grünhagen W (2004). *Inversion impossible?* Bremen, Germany: University of Applied Sciences, Technical Report, 2004.
42. Murray-Smith D J (2011). Feedback methods for inverse simulation of dynamic models for engineering system applications, *Mathematical and Computer Modelling of Dynamical Systems*. 2011; 17 (5): 515-541.Available online: http://eprints.gla.ac.uk/66825/1/66825.pdf Accessed 24/06/20.
43. Murray-Smith D J (1995). *Continuous System Simulation*, Chapman & Hall: London, UK. (Subsequently republished by Springer, ISBN 978-1-4615-2504-2).
44. Zenor J J, Murray-Smith D J, McGookin E W and Crosbie R E (2009). Development of a multi-rate simulation model of an unmanned underwater vehicle for real-time applications. *Simulation Notes Europe,* 2009; 19, 3-4: 47-54. (doi: 10.11128/sne.19.tn.09951). Available online:

https://www.sne-journal.org/sne-volumes/volume-19/sne-193-4-articles/development-of-a-multi-rate-simulation-model-of-an-unmanned-underwater-vehicle-for-real-time-applications Accessed 20/06/20.
45. Anonymous (2018). *W2W Zero Emissions Power System*. UK Research and Innovation, Gateway to Research Portal. Online: https://gtr.ukri.org/projects?ref=971637 Accessed 20/06/20.
46. Prentice S (2020). Personal communication – graphical data relating to Class 156 diesel multiple unit performance.

Appendix

Class 156 two-coach diesel multiple unit

The Class 156 diesel multiple unit was used to provide a point of reference in terms of performance because it is currently the type of unit used on routes such as the West Highland lines for train services from Glasgow to Oban, Fort William and Mallaig and also the services from Glasgow to Stranraer.

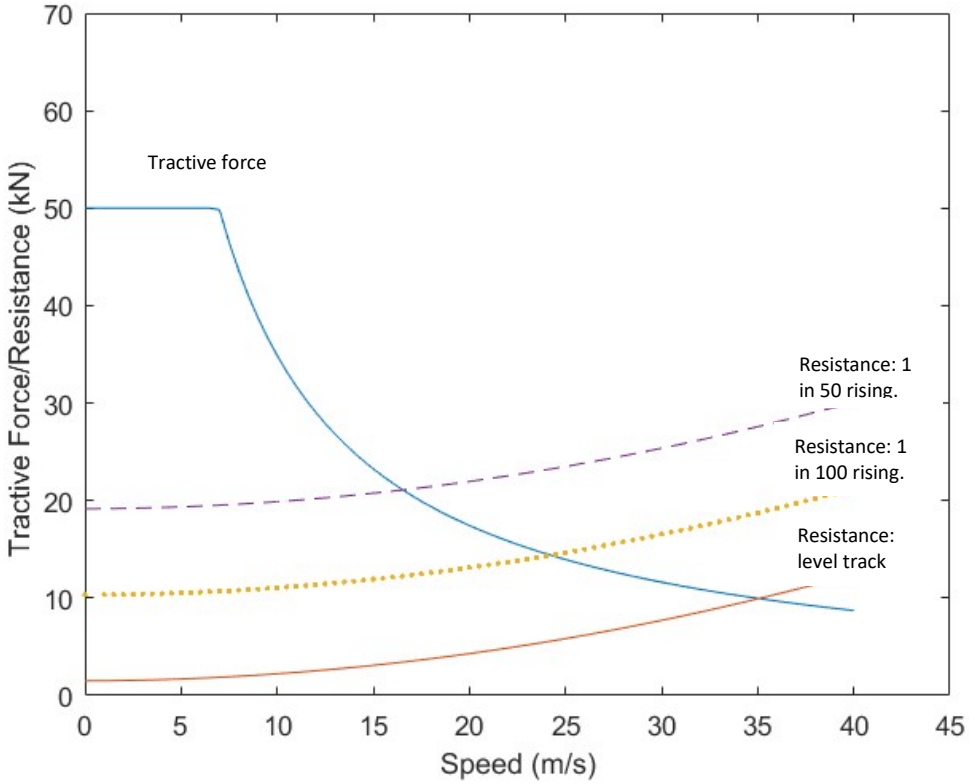

Figure A1: Tractive force and resistance cures for a Class 156 two-coach unit for three different cases involving level track (continuous line), a rising gradient of 1 in 100 (dotted lie) and rising gradient of 1 in 50 (dashed line). Parameter values T0=50,000 N, A=1500, B=0.006, C=0.0067, M=90,000kg, Power at rail=348.48 kW.

The mathematical model for a Class 156 diesel multiple is based on the train performance model of Section 2. The diesel engines and transmission system are modelled in the simplest possible way with the engines considered as an ideal power source. It is assumed that the auxilary power load is 30kW and this is subtracted from the available engine power before transmission. The transmission system efficiency is assumed to be 88%.

Figure A1 shows a set of characteristic curves for tractive force at the rail, T (kN), and resistive force at the rail R (kN) as a function of velocity $\dot{x}$ (m/s) for three different conditions in terms of the gradient for a two-car Class 156 diesel multiple unit for the parameter values of Table A1. The initial acceleration

is limited by the maximum tractive force of 50 kN at low speeds and the balancing speed conditions at which the tractive force is equal to the resistive force can be seen clearly. These balancing speeds are about 35 m/s in the case of level track, falling to slightly less than 25 m/s on a 1 in 100 rising gradient and to about 16 m/s in the case of a 1 in 50 rising gradient.

Table A1. Parameter values used in the simulation model for a Class 156 two-car diesel multiple unit

Quantity	Symbol	Numerical value with units
Engine power per 2-car unit	P_E	426 kW
Train mass (gross)	M	90,000 kg (90 tonnes)
Tractive force at zero speed	T_0	50 kN
Transmission efficiency	η	0.88
First resistance coefft.	a	1500 N
Second resistance coefft.	b	6.0 $Nm^{-1}s$
Third resistance coeff.	c	6.7 $Nm^{-2}s^2$
Gravitational constant	g	9.81 ms^{-2}
Power for auxiliaries	P_A	30 kW

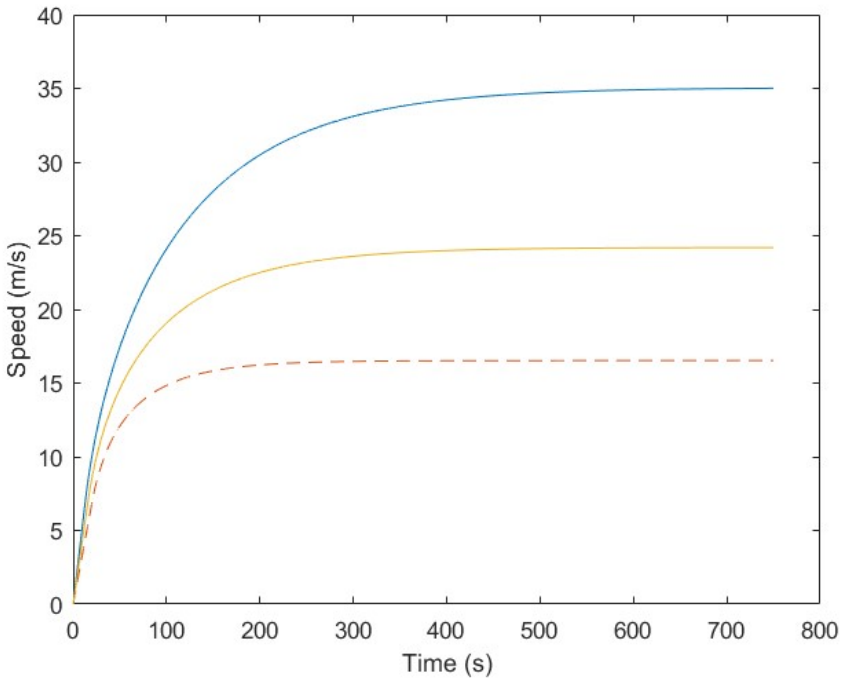

Figure A2: Simulation results for Class 156 two-coach diesel multiple unit for three different cases involving level track (continuous line, top curve), rising gradient of 1 in 100 (dotted line, middle curve) and rising gradient of 1 in 50 (dashed line, lowest curve).

Figure A2 shows results from simulation runs for the three different gradients considered above and these are consistent with the balancing speed values noted in the analysis of results in Figure A1. For example, the steady speed achieved in the simulation results for the 1 in 50 gradient of 16.53 m/s is consistent with the point of intersection of the tractive force curve and the dashed line representing the resistance for the case involving that gradient. The values in Figure A2 are also consistent with acceleration curves for Class 156 units included in data from the British Rail era [46] where steady-state balancing speeds are shown as equivalent to 34.7 m/s on the level, 24 m/s on a 1 in 100 rising gradient and 16.44 m/s on a 1 in 50 rising gradient. This suggests that the values assumed for the Davis resistance coefficients and the form of tractive force characteristics are appropriate.

Figure A3 shows simulation results in terms of speed versus time for the Class 156 simulation model for the route described in Section 3 for conditions in which the maximum available power is applied during the initial acceleration. The first phase, which involves acceleration on level track, is consistent with the corresponding simulation result in Figure A2 and is also consistent with the Class 156 acceleration curve for level track conditions [46]. The second phase involves steady running at the line limit of 60 mph (96 km/hr) before the start of the 1 in 50 rising-gradient, where speed falls significantly. A section of level track is reached at the top of the gradient and speed rises again to the line speed limit. Coasting starts at 12 km from the starting point and the brakes are applied progressively from 14.3 km until the train comes to a halt. During that final stage of the journey, when brakes are being applied the trajectory shows the initial deceleration of about 0.25m/s^2, increasing to about 0.6 m/s^2 in the final stage of braking. The braking force used in the simulation model involves a progressive frictional braking strategy in which the force applied is inversely proportional to the speed. In the final phase of braking, the braking force is taken to be equal to the tractive force value at the adhesion limit of 50 kN. It is of interest to note these simulation results are broadly consistent with available information concerning braking distance curves for Class 156 units [46], although the deceleration rate used in that case was greater (approximately 0.72 m/s^2) than the gentler braking strategy used here.

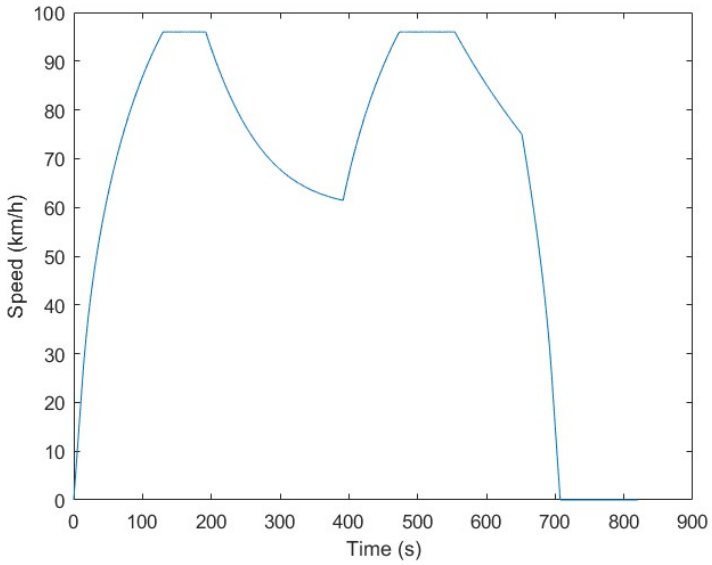

Figure A3: Simulation results for Class 156 two-coach diesel multiple-unit, for the route described in Section 3 in terms of speed (km/h) versus time (s).

Figure A4 shows the distance versus time plot corresponding to the speed versus time record of Figure A3. The train comes to a halt in 11 minutes and 48 seconds at a point 15 km from the start. The required power input values are shown in Figure A4 which shows that the maximum available power at the rail is applied during the acceleration phase and also on the rising gradient of 1 in 50. On level track, where speed is limited to 26.7 m/s (96 km/hr or 60 mph), the power required drops to about half of the maximum available. During the coasting phase the power level drops to zero, as may be seen from Figure A5. Braking force and power are shown with negative values in Figure A6 (tractive force) and, Figure A5 (power at the rail). As discussed above, the friction braking is applied at a power level equal (but opposite in sign) to the maximum power at the rail available from the diesel engines. The tractive force values shown in Figure A6 indicate that the starting tractive force is equal to the adhesion limit of 50,000 N and that the tractive force falls to a value less than 10,000 N during the periods when the train is running on level track at the line speed limit. The adhesion limit applies again during the final phase of braking.

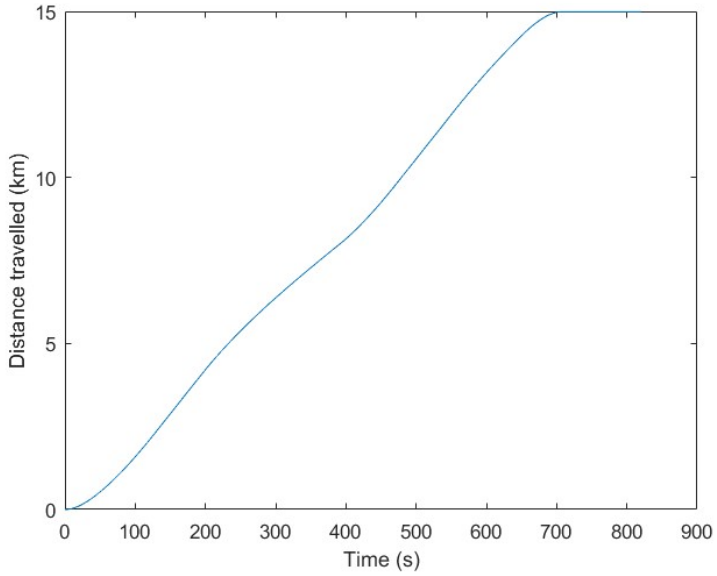

Figure A4: Simulation results for Class 156 two-coach diesel multiple unit, for the route described in Section 3 in terms of distance travelled (m) versus time (s).

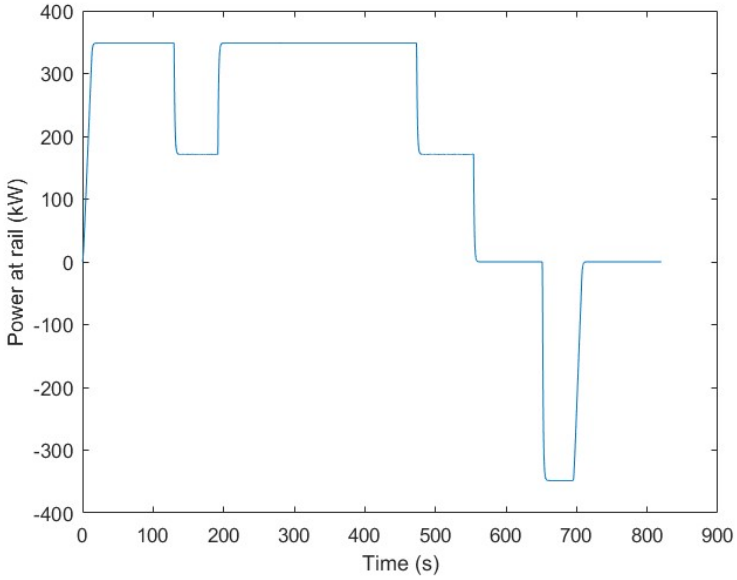

Figure A5: Simulation results for Class 156 two-coach diesel multiple unit for the route described in Section 3 in terms of power (kW) at the rail versus time (s).

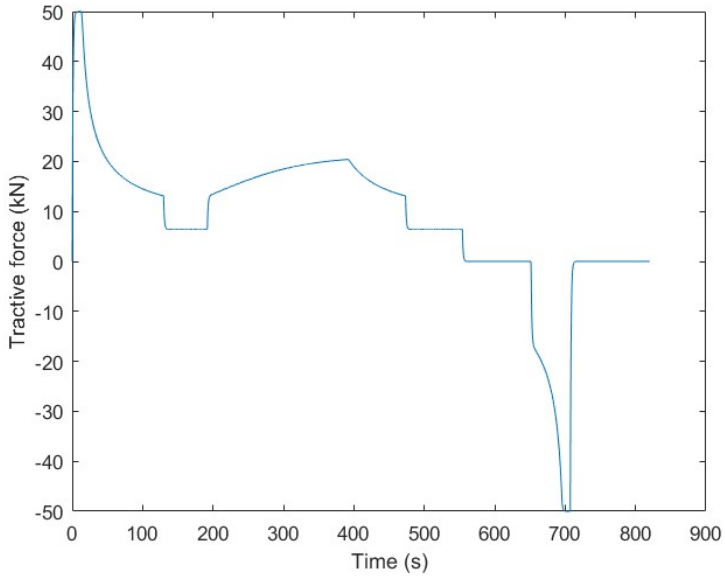

Figure A6: Simulation results for Class 156 two-coach diesel multiple unit for the route described in Section 3 in terms of tractive force (kN) at the rail versus time (s).